

Supplementary materials

Life-cycle assessment of Power-to-Liquid Kerosene produced from renewable electricity and CO₂ from Direct Air Capture in Germany

Matteo Micheli^{1,*}, Daniel Moore^{1,*}, Vanessa Bach¹ and Matthias Finkbeiner¹

¹ Department of Sustainable Engineering, Institute of Environmental Technology, Technische
Universität Berlin, Straße des 17. Juni 135, 10623 Berlin

* Correspondence: micheli.m.research@gmail.com (M.M); daniel.lochner@tu-berlin.de (D.M.)

The Supplementary Materials contains additional information on the methodological choices of the LCA (Section S1), overviews and information to the modeling of the background data (Section S2), a summary of the main assumptions of the LCA (Section S3) and the break-even points of CO₂ eq. emissions of PtL-kerosene (Section S4). An MS Excel file with all LCIA results is also available online.

The following table of contents shows the structure and detailed content of each section of the Supplementary Material.

Content

1. Methodological choices.....	4
1.1 Rationale behind preliminary methodological choices with an emphasis on the LCI.....	4
1.2. Overview of preliminary methodological choices with an emphasis on the LCI.....	4
1.3. System boundary.....	10
1.3.1. PtL-kerosene.....	10
1.3.2. Jet A-1.....	12
1.4. Geographical scope	13
1.5. Temporal scope	14
1.6. Technological scope	14
1.6.1. Foreground system.....	14
1.6.2. Background system	15
2. Modeling of background data	15
2.1. Non-renewable primary energy use.....	15
2.2 CO2 feedstock mass flow	16
2.3. PtL-plant: impacts from construction and EOL	17
2.3.1. GWP, EP, AP, POCP and non-renewable primary energy.....	17
2.3.2. Land transformation.....	21
2.3.3. Water consumption.....	22
2.4. PtL-plant: impacts from the use phase	22
2.4.1. Gas flaring.....	22
2.4.2. GWP, EP, AP, POCP, non-renewable primary energy, land transformation, indirect water consumption.....	23
2.4.3. Direct water consumption.....	23
2.5. PtL-plant, HTFT layout: electricity consumption of main processes	24
2.6. PtL-plant, HTFT layout: excess heat	26
2.7. PtL-plant, LTFT layout: Electricity consumption of main processes, water consumption and excess heat production	27
2.7.1. Electricity demand of the electric heater replacing the burner	28
2.7.2. Effects on the main mass and energy flows due to the removal of the burner	30
2.7.3. Water consumption.....	35
2.8. DAC plant: impacts from construction and EOL.....	35
2.8.1. GWP, EP, AP, POCP, and non-renewable primary energy.....	35
2.8.2. Direct land transformation	36
2.8.3. Indirect land transformation and water consumption.....	38
2.9. DAC plant: impacts from the use phase	39

2.9.1. GWP, EP, AP, POCP, non-renewable primary energy, land transformation, water consumption.....	40
2.9.2. Final energy consumption	41
2.9.3. Heat energy supply to the Climeworks plant coupled with the LTFT PtL-plant	43
2.9.4. Natural gas: GWP, EP, AP, and POCP.....	44
2.9.5. Natural gas: non-renewable primary energy and land transformation	44
2.9.6. Note on indirect land transformation and water consumption.....	45
2.10 Product system: water consumption	45
2.10.1. Direct consumption from electrolysis	46
2.10.2. On-site water production: water as a side product of the PtL-plant	46
2.10.3. On-site water production: water as a side product of DAC	47
2.10.4. Total direct water consumption	48
2.10.5. Indirect and total water consumption	48
2.11. Electricity from PV	48
2.12. Electricity from wind power	49
2.12.1. GWP, EP, AP, POCP, non-renewable primary energy and water consumption	49
2.12.2. Direct land transformation.....	50
2.12.3. Indirect land transformation	54
2.13. Electricity from the German electricity mix	55
2.14. PtL-kerosene: impacts	55
2.14.1. Production	55
2.14.2. Combustion	55
2.15. Jet A-1: impacts	57
2.16. Jet A-1: effects of renewable electricity on environmental impacts	57
2.17. Global aviation: tailpipe emissions share of stratospheric CO ₂	58
2.18. Water purifier and deionizer	59
2.19. Comparability of LCIA methods.....	60
2.20. Jet fuel	63
3. Overview of main assumptions and parameters	64
4. Break-even points of CO ₂ eq. emissions of PtL-kerosene.....	66
References	67

1. Methodological choices

This section describes the rationale and implications of preliminary methodological choices.

1.1 Rationale behind preliminary methodological choices with an emphasis on the LCI

The approach used in this work is LCA-based and adheres closely to the ISO standard (based on [1]), exception made for the LCI.

1.2. Overview of preliminary methodological choices with an emphasis on the LCI

A preliminary analysis of likely environmental impacts of PtL-kerosene and their hotspots is performed to meet preliminary methodological choices. A first analysis relies on the only published LCA study of an FT PtL-plant at the time of the literature review from Lozanovski and Brandstetter (2015) [2]. Preliminary methodological choices are counter-proofed with preliminary results and finalized, after common LCA practice [1].

Lozanovski and Brandstetter (2015) quantify GWP, AP, EP, POCP, and non-renewable primary energy consumption from e-Diesel production and use in a road vehicle using a WTW boundary and including all flows from upstream and downstream processes [2]. E-Diesel is produced in the same HTFT plant analyzed in the present work, is coupled with a DAC plant from the Swiss company Climeworks and operates at different final production electricity mixes in Germany in 2015.

The lower heating value (LHV) of e-Diesel (43.5 MJ/kg) is 2.7% lower than the LHV of PtL-kerosene (44.7 MJ/kg), making the energy weighted results in the work applicable to PtL-kerosene production (Lozanovski and Brandstetter (2015) only specify that the LHV of the liquid hydrocarbons produced (i.e. diesel, gasoline and kerosene) range from 43.5 MJ/kg to 44.7 MJ/kg [2]. Considering that the LHV diesel < LHV gasoline < LHV kerosene [4], it follows that the 43.5 MJ/kg is the LHV of diesel, while 44.7 is the LHV of kerosene from Lozanovski and Brandstetter (2015)). It is pointed out that according to a different study, the lower heating values of e-Diesel and PtL-kerosene produced via the FT pathway

differ by <0.05% (based on König et al. (2015) [3]). The findings of Lozanovski and Brandstetter (2015) are thus indicative of the environmental impacts that can be expected from PtL-kerosene produced via the HTFT pathway coupled with the Climeworks DAC plant.

Some of the results of Lozanovski and Brandstetter (2015) [2] are thus used to meet some methodological choices of the present work, namely:

- (i) The e-Diesel production plant's construction and end-of-life (EOL) phases cause negligible shares of the environmental impacts over the fuel's lifecycle, regardless of the final production electricity mix, exception made for the case where final fuel production energy is composed of wind and/or photovoltaic energy only. These results are based on the collection of primary data of the "Fuel 1" HTFT PtL-plant developed by the company Sunfire [5].
- (ii) The environmental impacts of e-Diesel are almost entirely caused during the **production and combustion phases of the fuel**. In the combustion phase, the environmental impacts are directly caused by the emissions to air. In production, **the environmental impacts are caused indirectly by the background processes** needed to produce and deliver the final electricity. The reason for the latter is that the production of e-fuel is a highly energy-intensive practice, requiring up to 2.2 MJ of electricity and 4.1 MJ of primary fossil energy per MJ of PtL-kerosene (own analysis. The values found by Lozanovski and Brandstetter (2015) are closely similar).

The considerations (i) and (ii) lead to the following observations.

From (i):

- (a) The environmental impacts from construction and EOL of the HTFT plant from the work of Lozanovski and Brandstetter (2015) are used in this work and adjusted for the difference in LHV between the fuels. Re-calculating them is assumed to not deliver

more accurate results, since these are based on primary data, and no other LCI data for the plant was available at the time of the literature review.

- (b) The environmental impacts from the construction and EOL phases of the LTFT plants are calculated based on the LCIA results of the Fuel 1 plant from the work of Lozanovski and Brandstetter (2015). Since no LTFT plant has been built at the time of the literature review and since the only major infrastructural difference between the plants is the type of electrolyser, this is considered to be the modeling choice delivering the estimates for associated LCIA results.

Additionally, even if this modeling choice arguably does not provide highly precise LCIA results, these are likely to comprise small shares of the lifecycle environmental impacts of the fuel. This may not be the case solely if the final production energy is electricity from wind power and/or PV only (see (i) above). Additionally, the electrolyser comprises 0.9% of total plant mass (based on [2]), and is thus very likely to contribute marginally to impacts from construction and EOL. Since the HTFT and LTFT plants analyzed in this work use the same types of processes, components other than the electrolyser is assumed to be similar, which increases the validity of applying the results of Lozanovski and Brandstetter (2015) to LTFT designs.

- (c) The inventory data of the Fuel 1 construction materials is considered to represent conservative mass estimates. The Fuel 1 plant is a demonstration plant that does not take advantage of upscaling effects due to a low production volume of 159 liters of liquid hydrocarbons per day. Commercial-scale PtL-plants with higher production volumes using the same main components as the Fuel 1 (i.e., as the PtL-plants studied in this work) can be expected to have smaller energy-specific material flows (e.g., kg steel/MJ fuel), and consequentially cause smaller environmental impacts associated with their construction and EOL phases. This is likely the case for the LTFT plants

studied herein since these have a production volume 1,000 times higher than the Fuel 1, for example compared to the production volume of 170 t/day in the theoretical LTFT plant described by König et al. (2015) [3].

From (ii):

- (d) From (ii), it follows that the environmental impacts of PtL-kerosene are mainly a function of four factors:
 - a. The environmental impacts of the production energy mix, which in turn are a function of the lifecycle environmental impacts of the single energy carriers,
 - b. and of their shares of final production energy.
 - c. The amount of final production energy (MJ/MJ, PtL-kerosene), which in turn is a function of the product system layout and operating conditions.
 - d. The environmental impacts of the combustion of PtL-kerosene, including the radiative forcing index (RFI).

Consequently, the focus of the LCA is put on maximizing the accuracy of the data pertinent to a. to d. To increase accuracy, the following choices are met:

1. The impacts of wind energy are mainly derived from an LCA study by wind turbine manufacturer Vestas, which comprised approximately 24% of the German wind power market by installed capacity in 2017 [6]. The LCA is based on primary data from Vestas and was audited externally [7].
2. The impacts of the PV system are calculated for the most used PV array type in Germany (polycrystalline modules) with the modules being sourced from the market leader in Germany, China (based on [8–11]) and with the most used layout worldwide (fixed axis,

i.e. without solar tracking ([12]). The main LCA study used as the source of the LCIA results is based on primary data from the Chinese polycrystalline PV industry [13].

3. The impacts of the German electricity mix are calculated with the LCA software GaBi based on Sphera's LCI database [14].
4. The impacts of natural gas are calculated based on a review study of primary energy factors in Germany [15], and a LCA study of the German electricity and gas sector [16].
5. The final energy consumption of the product system is calculated from primary data or from a theoretical PtL-plant model from literature. Specifically:
 - a. The final energy consumption of HTFT and LTFT plant operation is mainly calculated from data obtained through correspondence with Sunfire and from a theoretical LTFT design model developed in a doctoral dissertation on PtL-kerosene production from CO₂ and hydrogen in cooperation with the German Aerospace Center (DLR) [3].
 - b. The data on final energy consumption of the DAC plants is derived from one peer-reviewed article written by the technical lead and founder of Carbon Engineering [17]. The Carbon Engineering DAC plant also analyzed in this work. For the Climeworks plant, the data is derived from Viebahn et al. (2019) [18].
6. All values are integrated into a spreadsheet where the impacts are calculated as a function of three variables (plant type, plant layout, and final energy mix composition) which can be adjusted to analyze any scenario.
7. The impacts of PtL-kerosene combustion are quantified based on laboratory tests on FT-PtL-kerosene combustion [19], and are checked against other literature [20,21].

Additionally, the RFI is calculated based on a systematic review study of RFI calculation methods and is checked against other further literature [22,23].

8. Land transformation requires dedicated attention and is discussed below.

Land transformation is divided into two components: land transformation **directly** caused by the infrastructure of the process or flow and land transformation **indirectly** caused by upstream and downstream processes of the process or flow.

An effort is made to consider both components of land transformation for all foreground and background processes. For some processes, no data was found. Nonetheless, both components are quantified for all energy carriers.

Sphera has recently updated its methodology to quantify land transformation to the LANCA method [24]. Upon request, Sphera has confirmed that in this method, only upstream contributions to the land transformation of the German electricity mix and Jet A-1 produced in Germany are quantified. This means that the land transformation from power plant infrastructure is not included in the GaBi databases (for the German electricity mix and Jet A-1).

For the German electricity grid mix as a whole, not considering the contribution of the power plant infrastructure does not have a strong influence on the absolute land transformation of the system, since the provision of biomass and biogas alone comprise 97% of the impact, and are notoriously land-use intensive practices [25], meaning that the ratio of direct land transformation over indirect land transformation is assumed to be negligible.

For electricity from PV and wind, land transformation from the power plant itself has the same order of magnitude of indirect land transformation, mainly from upstream processes (as found in this work. See 2.11). Therefore, both contributions must be considered. This is especially important in this work since the environmental impacts of PtL-kerosene are predominantly a function of the final production energy mix.

Direct land transformation for PV and wind electricity is calculated through own models based on literature data. The indirect contributions are obtained from the GaBi database, 2019 version, for Germany with the reference year 2015 [14].

Combining upstream data from GaBi with own calculations may not provide highly accurate results. For example, the PV system modeled herein is based on polycrystalline PV panels arranged in an array with no solar tracking mechanism. The upstream data from GaBi includes all different PV systems installed in Germany and is thus only partially representative of the modeled system.

Wind energy is here modeled based on a 50 MW onshore wind farm using 2 MW Vestas turbines. The same rationale regarding indirect land transformation depicted for the PV system applies here, too.

The values of indirect land transformation for the following flows from the cited GaBi database are used: electricity from wind power, electricity from PV, natural gas, and Jet A-1 [14].

The year of reference is set to 2015 to allow a comparison with the only comprehensive LCA on e-fuels available to date [2] and to allow to use part of the inventory data used by Lozanovski and Brandstetter (2015).

1.3. System boundary

1.3.1. PtL-kerosene

For clarity, an overview of the studied subsystems and flows classified by the lifecycle stages of PtL-kerosene is provided in Table S1. The system boundary is displayed in Figure S1. Background and foreground processes are highlighted. Figure S1 also shows that some products need to be allocated. Table S2 shows the system boundaries by subsystem by lifecycle stages. The system boundary is displayed in Figure S1. Background and foreground processes are highlighted. Figure S1 also shows that some products need to be allocated. The system boundary and related material and energy flows for the use phase of the production plant at a foreground system level are displayed in Figure 1 of the main paper.

Table S1. Subsystems and flows included in the study of the impacts from the lifecycle stages of PtL-kerosene

Subsystems and flows studied by lifecycle stages of PtL-kerosene		
	Lifecycle stage	
	WtP	PtWa
Included subsystems or flows	PtL-plant	Combustion process
	Carbon capture plant	
	Electricity from the German el. Mix	
	Electricity from Wind power	
	Electricity from the PV array	
	Natural gas	
	Electricity and heat from natural gas	
	Water	

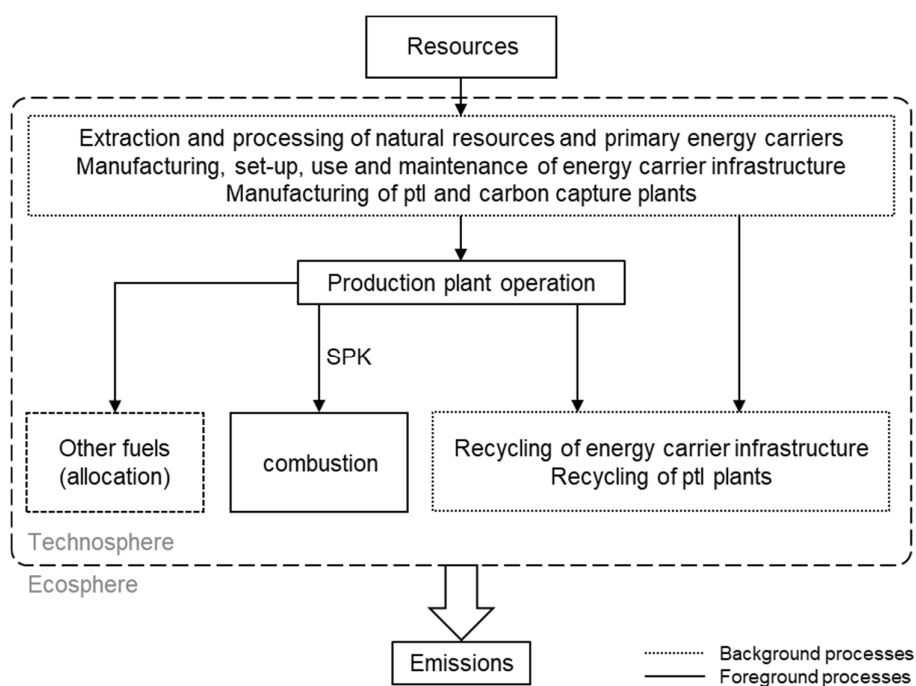


Figure S1. System boundary, highlighting the foreground and background systems

Table S2. System boundaries by subsystem or flow of the product system by lifecycle stage

System boundaries by subsystem or flow					
Grouping	Subsystem or flow	Lifecycle stage			
		Manufacturing (or extraction)	Operation (or use)	Maintenance	EOL
PtL-plant	HTFT plant	✓	✓ _{NEG}	✗ _{NA}	✓
	LTFT plant	✓	✓ _{NEG}	✗ _{NA}	✓
Carbon capture plant	DAC plants (Carbon Engineering and Climeworks)	✗ _{NA}	✓ _{NEG}	✗ _{NA}	✗ _{NA}
Final energy source	German el. mix	✓	✓	✓	✓
	Wind power	✓	✓	✓	✓
	PV array	✓*	✓ _{NEG}	✓ _{NEG}	✓
	Natural gas	✓	✓	(-)	(-)
Water	Water	✗	✓	(-)	(-)
Vehicle	Aircraft	(-)	(As fuel use)	(-)	(-)
Fuel	PtL-kerosene	✓	✓	(-)	(-)
	Jet A-1	✓**	✓	(-)	(-)

NA = no data available; NEG = Negligible; (-) = does not apply or is outside of the scope; *upstream emissions from the production plant are not included since negligible according to the source; ** impacts of EOL practices from the fuel production plant are not included (see section 1.3.2.).

1.3.2. Jet A-1

The system boundary of the refinery model is shown in Figure S2 and takes upstream processes associated with the input flows into account, but not end-of-life processes. For a more detailed description of the model, the reader is invited to refer to [27].

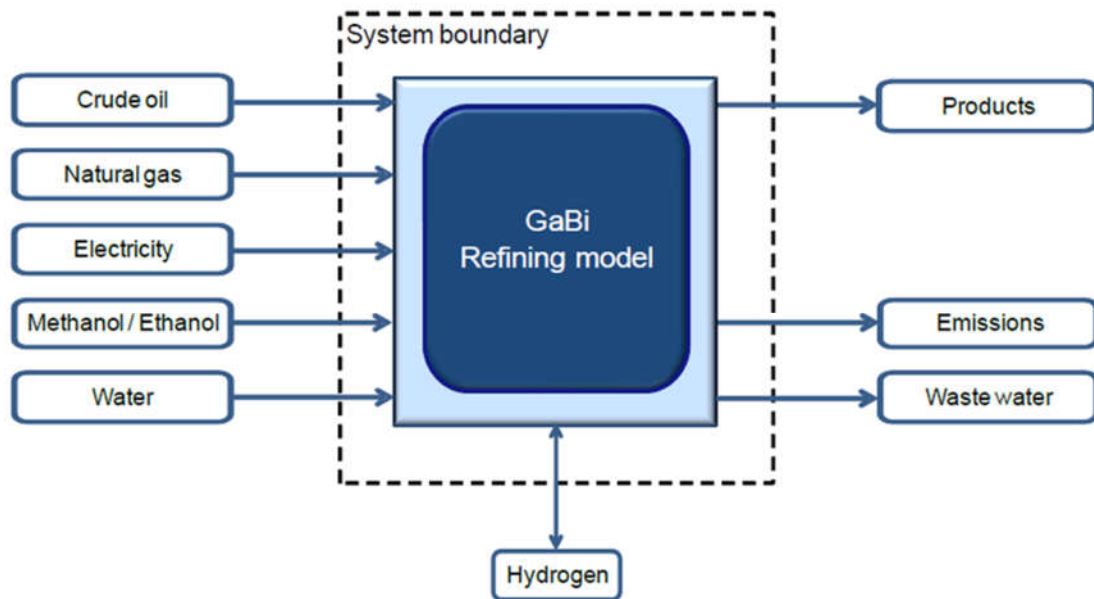


Figure S2. GaBi refinery model system boundary [27]

1.4. Geographical scope

The geographical scope for both fuels is set to Germany and the results are strictly valid for this region only.

1.5. Temporal scope

It is found useful to aggregate results as presented in Table S3 for readability.

Table S3. Geographical and temporal scope of the LCA by life cycle stage of main processes

Process or flow	Geographical scope	Temporal scope
PtL-plant* <i>construction and EOL</i>	Germany, up to mainland Europe	2015 – 2020
DAC plant** <i>construction and EOL</i>	n.a.	n.a.
Natural Gas <i>extraction and use</i>	Germany	2015 – 2020
Electricity from PV, <i>entire lifecycle</i>	Germany, up to mainland Europe	2015 – 2020
Electricity from wind power, <i>entire lifecycle</i>	Germany, up to mainland Europe	2015 – 2020
Electricity from the German el. Mix, <i>entire lifecycle</i>	Germany	2015 – 2020
PtL-plant* <i>operation including related background processes</i>	Germany, up to mainland Europe	2015 – 2020
DAC plant** <i>operation including related background processes</i>	Germany, up to mainland Europe	2015 – 2025
Fuel (PtL-kerosene and Jet A-1) <i>combustion</i>	Worldwide	2015 – 2050
Water <i>extraction</i>	Germany, up to mainland Europe	2015 – 2020
Jet A-1 <i>production</i>	Germany	2015 – 2021

*applies to both HTFT and LTFT plants; **applies to both Climeworks and Carbon Engineering plants.

As for Jet A-1 production, the temporal scope indicated by the source spans from 2015 to 2021 [30].

1.6. Technological scope

1.6.1. Foreground system

The different layout options allow to analyze a product system that operates at typical energy conversion efficiencies achievable today, as well as at likely best-case efficiencies reachable in the upcoming years.

The HTFT model represents the “Fuel 1” PtL demonstration plant developed by the German company Sunfire GmbH, operational since 2014, which has received increased attention as a viable HTFT design from industry (as for example mentioned by Searle and Christensen (2018) [31] and Deutsche Energie-Agentur GmbH (dena) [32]). For clarity, it is pointed out that a carbon capture plant is not part of the Fuel 1.

The LTFT plant design is adapted from a theoretical design employed in PtL-kerosene production from CO₂ and hydrogen, developed with the DLR [3]. This design is used to create a plant model using PEM, one of the most common electrolyser types worldwide besides SOEC [33,34].

The PtL-plants’ impacts are calculated from primary data and literature data [2,3,18,24,35–50].

The impacts from heat demand, under consideration of the use of excess heat from other processes, are quantified based on the digression in section 2.9.3.

1.6.2. Background system

The background system is modeled using literature data and the GaBi database. The data sources represent state of the art technologies employed in Germany, or provide a conservative picture of them, given that some data is up to 8 years old. This aspect is elaborated upon in detail in section 2.

2. Modeling of background data

Part of the processes, flows, and components of the product system and/or part of their environmental impacts are modeled based on literature values to produce the background data upon which the environmental impacts of the product system are calculated.

2.1. Non-renewable primary energy use

Table S4 shows the sources used to quantify non-renewable primary energy, and of the type of inventory data used in the sources, by process or flow.

Table S4. Overview of the sources used to quantify non-renewable primary energy, and of the type of inventory data used in the sources, by process or flow

Overview of the sources used to quantify non-renewable primary energy, and of the type of inventory data used in the sources, by process or flow		
Process or flow	Inventory data type	Reference
HTFT plant construction and EOL	primary (I)	[2]
LTFT plant construction and EOL	primary (I)	[2]
DAC plant construction and EOL	primary (I)	based on [2]
Natural Gas entire lifecycle	primary (I)	[15,16]
El. from PV entire lifecycle	primary (I)	[13]
El. from wind power entire lifecycle	primary (I)	[7]
El. from German el. mix entire lifecycle	GaBi db, 2019	[14]
Jet A-1 production	GaBi db, 2019	[14]
PtL-kerosene production	Calculated within this work	

(I) = from literature; El. = Electricity

2.2 CO₂ feedstock mass flow

The amount of carbon dioxide needed to produce PtL-kerosene is calculated starting from the combustion products of fossil kerosene.

First, it must be noted that CO₂ makes up 99.9% (w/w) of carbon-containing molecules in the combustion gas of the fuel [21]. Second, as discussed in 2.14, the same amount of CO₂ per kg of fuel is emitted to air in FT PtL-kerosene and Jet A-1 combustion alike. Third, considering that the gravimetric energy density of Jet A-1 (43.2 MJ/kg) is 2.5% lower than in PtL-kerosene (44.1 MJ/kg), the CO₂ emissions per unit energy are 2.5% lower in PtL-kerosene (based on [26]).

Lastly, the combustion of Jet A-1 causes 73.25 g CO₂/MJ [14], thus the tailpipe CO₂ emissions of PtL-kerosene amount to:

$$Tailpipe\ CO_2, SPK = 0.975 \cdot 73.25 \left[\frac{gCO_2}{MJ, SPK} \right]$$

According to Lozanovski and Brandstetter (2015) [2], no carbon dioxide is lost between capture and binding in the hydrocarbons of the final fuel, and thus no carbon is lost. Here, a more conservative approach is taken, assuming a 5% difference between the number of carbon atoms in the captured CO₂ feed stream and their amount in the final fuel. Consequentially, the quantity of feedstock CO₂ amounts to:

$$Feedstock\ CO_2, SPK = 1.05 \cdot Tailpipe\ CO_2, SPK = 75.0 \left[\frac{gCO_2}{MJ, SPK} \right].$$

2.3. PtL-plant: impacts from construction and EOL

Table S5. Overview of the addressed objects, lifecycle phases and indicators in section 2.3.

Applies to	
Object(s):	HTFT plant, LTFT plants
Lifecycle phase(s):	Construction, EOL
Indicator(s):	GWP, EP, AP, POCP, non-renewable primary energy, land transformation, and water consumption

The approach used to quantify the impacts of the PtL-plant (which includes the refining processes) is here discussed.

2.3.1. GWP, EP, AP, POCP and non-renewable primary energy

GWP, EP, AP, POCP as well as non-renewable primary energy consumption caused by the construction and EOL phases of the Fuel 1 plant and attached refining processes (i.e. the HTFT plant herein) are quantified by Lozanovski and Brandstetter (2015) [2] and indicated per MJ of produced fuel (e-diesel). These are here scaled on the LHV of PtL-kerosene based on the difference in LHV between the fuels (as discussed in 2.14).

It is here further argued that these values represent a conservative estimate for an LTFT design and are thus valid for such designs as well. This is complemented by the observations in section 2.7, in which the LTFT plant design is qualitatively described in more detail.

This hypothesis is based on the observation of the composition of construction materials employed in the Fuel 1 plant. An overview is provided in Figure S3 and Figure S4, a detailed inventory can be found in [2].

This poses a considerable approximation in terms of lifecycle thinking, since it is assumed that similar inventories apply to distinct systems (the HTFT and LTFT plants). This choice is made since no other LCA study at the time of the literature review quantified environmental impacts from the construction and EOL of LTFT plants comparable to the one herein, and because no inventory data of LTFT plants were found (Ecoinvent 3.6, GaBi 2019, JRC and US federal LCA commons were searched), nor plans detailing the size of components employed in LTFT plants, which could be used to compile an LCI.

Given the considerations above and the considerations on the comparability of the plants, this rationale is assumed to deliver representative results.

Additionally, it is pointed out that for each environmental impact, the construction and EOL phases are responsible for < 5% of the impact's magnitude regardless of the electricity mix¹, as is suggested by Lozanovski and Brandstetter (2015) [2] and found through a preliminary analysis performed in this work.

Concrete and steel comprise 94% of the plant's total mass of 479 tons. Both concrete and steel manufacturing are energy-intensive and fossil energy intensive processes. 16.6 GJ of final energy are consumed on average per ton of crude steel produced in Germany and 92% of the employed final energy is fossil².

¹ except for the case where electricity from wind energy > 75% of final electricity and the remainder is provided by the German national grid, where the contribution of the construction phase to POCP rises to up to 7%.

² Similar average values have been identified for Mexico, China and the U.S. in the cited work.

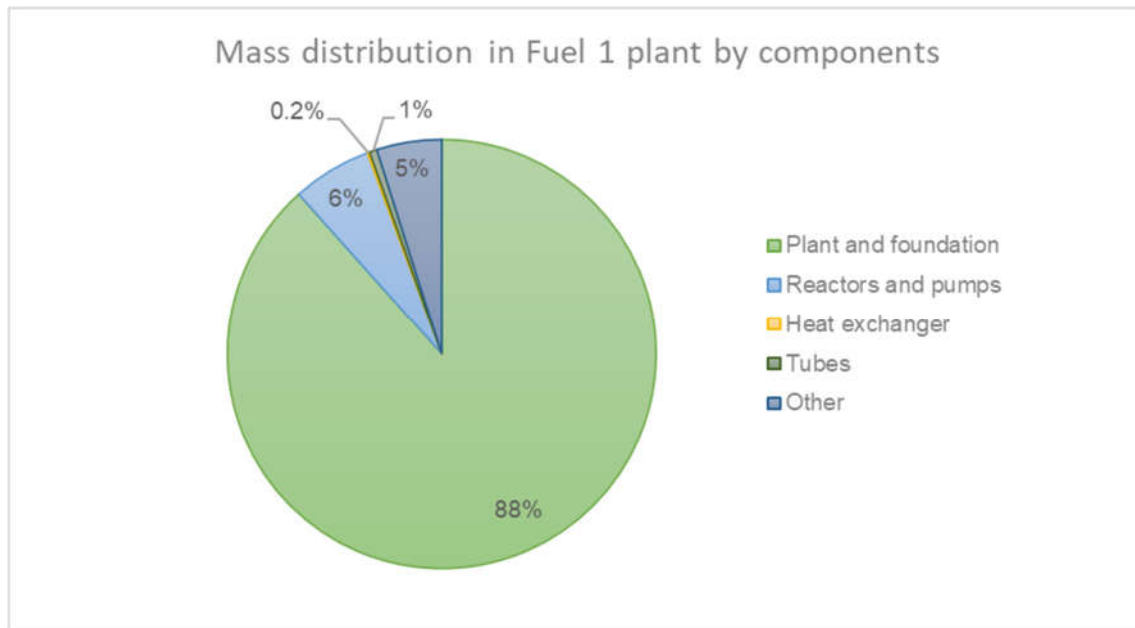


Figure S3. Mass distribution in Fuel 1 plant by components (based on [2])

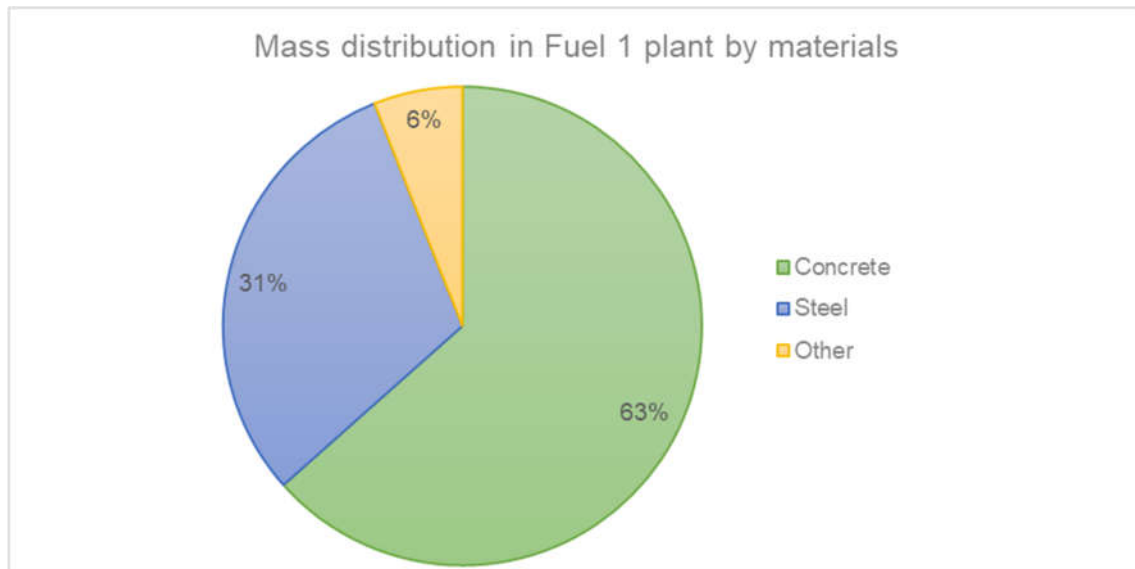


Figure S4. Mass distribution in Fuel 1 plant by type of materials (based on [2])

This caused an average 1.6 tons of CO₂ per ton of crude steel in Germany in 2010 [45].

Cement is too a highly energy intensive good with a high rate of specific fossil energy consumption comprising 90% of final production energy at approx. 2.8 GJ per ton of cement [46]. Furthermore, its production process causes non-primary energy specific CO₂ emissions through the decomposition of

carbonates. Total CO₂ emissions from cement production are estimated at around 1.1t CO₂ per ton of cement, independently from the location of production [47].

Besides CO₂ emissions, the combustion of hydrocarbons causes emissions which contribute strongly to GWP, AP, EP and POCP as can be concluded from the findings of Lozanovski and Brandstetter (2015) [2].

These observations imply that the cited environmental indicators and the primary energy associated with the construction of the Fuel 1 plant are dominated by the production of steel and concrete and are marginally influenced by construction practices.

The cited literature suggests that the production energy for steel and concrete is almost entirely of fossil origin. Additionally, the mentioned observations are valid for averages calculated upon the different plant designs in use today in Europe and beyond. Consequentially, the associated specific environmental impacts are assumed constant regardless of the origin of steel and concrete, across Europe.

EOL practices are considered by Lozanovski and Brandstetter (2015) [2] and include a recycling rate of 80% (w/w) of the metals used in the plant by discounting their impacts in accordance to World Steel Association [49] and European Aluminum Association [48]. In this approach, the environmental burdens associated with the production of 20% of the employed metals are charged to the product system, together with the burdens of the recycling operations.

EOL practices are assumed to be equal for both HTFT and LTFT plants and the differences between their impacts to be negligible. This is because the types of components of the plants making up about 95% of the plant's mass are identical³, from which follows the assumption that the amount of materials per unit product (e.g., kg steel/MJ, PtL-kerosene) is highly similar in both designs. Additionally, one LCA study found that AP, EP, GWP and POCP from the construction phase of PEM electrolyzers are 30% -

³ i.e., all but the electrolyser, which comprises 2.9% (w/w) of the Fuel 1 plant, and considering uncertainties due to the difference in the exact size of the components making up the plants (based on Lozanovski and Brandstetter (2015) [2]).

60% lower than for SOEC electrolyzers, per unit mass of hydrogen [50], which increases the validity of the above.

One additional difference in infrastructure between the two plant types worth analyzing is the size of heat exchangers, due to the different amount of recovered heat (lower in the LTFT plant). Heat exchangers are almost entirely made of stainless steel (99% (w/w) following from Alfa Laval (2017) [35]). The heat exchanger of the Fuel 1 plant makes up 2.4% (w/w) of the total amount of steel used in the plant (see Lozanovski and Brandstetter (2015) [2]). In accordance to Hasanbeigi et al. (2016) [45], it is assumed that environmental impacts from steel production for the heat exchanger do not differ significantly from the mean environmental impacts resulting from the production of the other kinds of employed steel (accounting for the remaining 97.6% (w/w) of steel employed in the plant). The LTFT plant operates at lower temperatures compared to the HTFT plant, and thus requires a smaller heat exchanger compared to the one employed in the Fuel 1 plant. This consequentially implies a smaller amount of employed steel, and thus of environmental impacts. Given the small amount of steel employed in the heat exchanger in the HTFT plant, this difference is assumed to have negligible effects on the overall results.

In conclusion, the environmental impacts and primary energy quantified by Lozanovski and Brandstetter (2015) [2] for the construction and EOL phases of the Fuel 1 plant are assumed valid for the LTFT and HTFT plants studied herein.

2.3.2. Land transformation

The land-use of the PtL-plants (any layout) is assumed to be equal to the amount of area A (Fuel 1) required by the Fuel 1 plant. This is considered a reasonable assumption, considering that there are virtually no structural differences between the different PtL-plants as discussed in the previous section.

For a production capacity of 100 million liters of final fuel per year, this amounts to:

$$A_{Fuel\ 1} = \frac{16,000}{100 \cdot 10^6} \left[\frac{m^2}{\frac{l}{a}} \right]$$

Under the conservative assumption that the transformed land is transformed indefinitely, and that it was of higher quality before the installation of the plant, A (Fuel 1) classifies as positive land transformation as defined by Sphera [24].

This is a conservative assumption, as the change in the quality of land can be expected to be different from project to project depending on the installation site, implying that land quality is not necessarily degraded.

Converting for the specific energy of PtL-kerosene and considering the plant's operational life of 20 years [2], the above translates to:

$$\text{Land Transformation PtL, direct} = 2.42 \cdot 10^{-7} \left[\frac{m^2}{MJ} \right].$$

Indirect land transformation from the construction and EOL phases is unknown. It is **assumed negligible**, since the product system consumes high amounts of energy during operation, causing a high amount of indirect land transformation ascribed to the energy carriers.

2.3.3. Water consumption

The amount of water consumed during the construction and EOL phases of the PtL-plants is unknown. It is **assumed negligible**, given that the product system consumed extensive amounts of water during operation.

2.4. PtL-plant: impacts from the use phase

Table S6. Overview of the addressed objects, lifecycle phase and indicators in section 2.4.

Applies to	
Object(s):	PtL-plant, all layouts
Lifecycle phase(s):	Use
Indicator(s):	GWP, EP, AP, POCP, non-renewable primary energy, water consumption, land transformation

2.4.1. Gas flaring

A gas flare is a required component in a refinery to guarantee safe operation and minimize atmospheric emissions. It causes direct emissions during fuel production, as it burns excess gases from the refining

process with an emission profile similar to burned natural gas [2]. In their analysis, Lozanovski and Brandstetter (2015) [2] conclude that gas flaring has negligible impacts on each of the analyzed environmental indicators (GWP-100, AP, EP, and POCP). This is thus assumed here valid, too.

2.4.2. GWP, EP, AP, POCP, non-renewable primary energy, land transformation, indirect water consumption

The environmental impacts caused over the lifecycle of the electricity carriers, as well as the associated non-renewable primary energy, land transformation and water consumption are ascribed to the use-phase of the PtL-plant.

The final electricity mix is comprised of electricity from three sources (PV (PV), wind power (Wind), and the German electricity mix (DE mix)) at different shares, adding up to 100%. Each impact I_i, Ptl attributed to the use-phase of the PtL-plant is calculated as the sum of the impacts I_{ij} of each electricity carrier j , weighted by their share s_j of the final electricity mix, multiplied by the electricity consumption E_{el, Ptl_k} of the PtL-plant in its layout k .

$$I_{i, Ptl_k} \big|_{i,k=const.} = E_{el, Ptl_k} \sum_j I_{ij} \cdot s_j$$

$$I_{i, Ptl_k} \big|_{i,k=const.} = E_{el, Ptl_k} (I_{i,PV} \cdot s_{PV} + I_{i,Wind} \cdot s_{Wind} + I_{i,DE mix} \cdot s_{DE mix})$$

With the corresponding units:

$$\left[\frac{kg}{MJ, SPK} \right] = \left[\frac{MJ, el}{MJ, SPK} \right] \left[\frac{kg}{MJ, el} \right]$$

Where:

- I_i = GWP, EP, AP, POCP, non-renewable primary energy, land transformation, indirect water consumption.
- j = Electricity from PV, wind power or the German electricity mix.
- k = HTFT plant operating at 80% efficiency, LTFT plant with PEM electrolysis.

2.4.3. Direct water consumption

Direct water consumption is discussed in 2.10

2.5. PtL-plant, HTFT layout: electricity consumption of main processes

Table S7. Overview of the addressed objects, lifecycle phases and indicators in section 2.5.

Applies to	
Object(s):	PtL-plant, HTFT layout
Lifecycle phase(s):	Use
Indicator(s):	GWP, EP, AP, POCP, non-renewable primary energy, water consumption, land transformation

The electricity consumption of the HTFT plant and of its main processes is here quantified. This allows to calculate the environmental impacts caused indirectly from the energy carriers and attributed to the use-phase of the plant. It is further needed to allow for an environmental hotspot analysis.

The overall electricity consumption of the plant is a function of its operational efficiency. The operational efficiencies for the HTFT plant analyzed in this work are 65% and 80%, which translates to 1.54 MJ/MJ, PtL-kerosene and 1.25 MJ/MJ, PtL-kerosene respectively.

The electricity demand of the SOEC electrolyser and RWGS reactor can be calculated from the reaction enthalpy of the power-to-liquid process steps [36,37] shown in

Table S8. These comprise the whole power to liquid reaction chain.

Table S8. Power-to-liquid chemical process steps and enthalpy of reaction (based on [36,37])

Power-to-liquid chemical process steps and enthalpy of reaction		
Process step	Reaction	Enthalpy ΔH [kJ/mol]
Evaporation	$3 \text{ H}_2\text{O (l)} \rightarrow 3 \text{ H}_2\text{O (g)}$	+ 141
SOEC electrolysis	$3 \text{ H}_2\text{O (g)} \rightarrow 3 \text{ H}_2 + 1,5 \text{ O}_2$	+ 726
RWGS reaction	$3 \text{ H}_2 + \text{CO}_2 \rightarrow 2 \text{ H}_2 + \text{CO} + \text{H}_2\text{O}$	+ 41
FT – synthesis	$2 \text{ H}_2 + \text{H}_2\text{O} + \text{CO} \rightarrow \text{CH}_2 + 2\text{H}_2\text{O}$	- 147

(l) = liquid, (g) = gaseous

Knowing the enthalpy of reaction, the Gibbs function allows to estimate the amount of electrical energy needed by each process. In its simplified form $\Delta H = \Delta G + T\Delta S$, it translates to change in enthalpy = electrical energy + thermal energy. The exothermic FTS reaction releases heat, which is

recovered and used to evaporate water. In accordance with Posdziech et al. (2017) [37], it is assumed that the remaining 6 kJ/mol of thermal energy are not recovered. This allows to calculate the shares of electricity consumed by the electrolyser and RWGS reactor at 94.5% and 5.5% of the total electricity consumed for these two processes respectively.

Additional electricity is required for fuel refining and compression processes (for CO₂ and steam). This data is not available for the Fuel 1 plant, but it is quantified by from König et al. (2015) [3] in his LTFT plant model. The electricity demand from compression and refining processes per unit product (energy based) is assumed equal in both plant types, since the energy specific flows are identical in both designs (i.e., kg H₂, kg CO₂ and consequently kg Syncrude per MJ of PtL-kerosene).

In the LTFT designs employing PEM electrolysers, the refining processes require 0.002 MJ of electricity per MJ of PtL-kerosene, while compression processes require 0.033 MJ of electricity per MJ of PtL-kerosene (see Table S9).

Combining the information above, following values for electricity consumption in the HTFT plant can be summarized. It is assumed that in the more efficient HTFT layout, the efficiency gains are equally distributed across all processes⁴.

Table S9. Electricity consumption in the HTFT plant by main process steps

Electricity consumption in the HTFT plant						
Energy conversion efficiency	Total	Electrolysis	RWGS reactor	Compression	Refining	Unit
65%	1.54	1.423	0.0804	0.033	0.002	$\left[\frac{MJ}{MJ, SPK} \right]$
80%	1.25	1.156	0.065	0.027	0.002	$\left[\frac{MJ}{MJ, SPK} \right]$
Shares	100.0%	92.50%	5.22%	2.15%	0.13%	-

⁴ This is an approximation, as it is more likely that efficiency gains are rather caused by decreased energy demand in the electrolyser and RWGS reactor, being technologies under development. Nonetheless, since those two processes consume > 97% of final energy, this approximation has negligible effects on the overall results.

2.6. PtL-plant, HTFT layout: excess heat

Table S10. Overview of the addressed object, lifecycle phases and indicators in section 2.6.

Applies to	
Object(s):	Climeworks DAC plant
Lifecycle phase(s):	Use
Indicator(s):	GWP, EP, AP, POCP, non-renewable primary energy, water consumption, land transformation

The amount of excess heat produced by the HTFT PtL-plant is here discussed. Here too, the Sunfire Fuel 1 plant serves as reference plant for calculations.

For this work, the relevant question is whether enough excess heat from the PtL-plant can be recovered in order to operate the Climeworks DAC plant in its 2019 layout. Based on literature, it is argued that this is the case when a HTFT layout is in place.

In the model of Lozanovski and Brandstetter (2015), the Fuel 1 plant is coupled with the Climeworks DAC plant [2]. In such a configuration, Lozanovski and Brandstetter (2015) state that while as of 2014 it was not possible to recover enough excess heat from the Fuel 1 plant to cover the thermal energy consumption of the Climeworks DAC plant due to design constraints, this could improve in future designs [2].

As of 2019, according to Viebahn et al. (2019) [18], the thermal energy required by the Climeworks DAC plant could be sourced entirely from a FTS plant.

Based on these two considerations, it is assumed that enough excess heat from the HTFT plant can be recovered to cover the heat demand of the Climeworks DAC plant.

It is further assumed that the effect on the studied indicators from modifications to infrastructure needed to increase the amount of recovered heat are negligible. The same rationale regarding the materials, mass and environmental impacts from construction and EOL of the PtL-plant laid out in 2.3. is here valid.

2.7. PtL-plant, LTFT layout: Electricity consumption of main processes, water consumption and excess heat production

Note: the following observations are based on an LTFT plant employing a PEM electrolyser.

Table S11. Overview of the addressed objects, lifecycle phases and indicators in section 2.7.

Applies to	
Object(s):	LTFT PEM plant
Lifecycle phase(s):	Use
Indicator(s):	GWP, EP, AP, POCP, non-renewable primary energy, water consumption, land transformation

In order to calculate the environmental impacts of the use-phase of the LTFT plants and the amount of land transformation, their energy and water consumption must be known. Energy and water consumption is calculated through further modeling of a flowsheet process model of an LTFT plant from literature [3]. In the model, hydrogen from a PEM electrolyser and CO₂ are used as production feedstock for PtL-kerosene.

The flowsheet process model is first checked for comparability with the Fuel 1 plant. This allows to ensure that the environmental impacts from the two plant types are comparable. The Fuel 1 plant and the LTFT plant model are considered comparable if two criteria are met:

- (a) the plant's infrastructure allows for the use of the same type of final energy and
- (b) both plants use the same main processes, and thus the same main components.

A detailed plant layout of the Fuel 1 plant is not publicly available, but an inventory of its main components aggregated by their function is provided by Lozanovski and Brandstetter (2015) [2]. As for the LTFT plant model, a flowsheet of the LTFT plant provides a detailed overview of the plant's components (see König et al. (2015) [3]).

A comparison shows that both types of plants employ the same main components. König et al. (2015) further quantifies their energy consumption [3]. The main infrastructural difference is the type of electrolyser (the influence of this difference on the environmental impacts is discussed in 2.3).

One significant difference is the energy provision of the RWGS reactor. In the Fuel 1 plant it is electric, while in the model of König et al. (2015) it is thermal, requiring 0.7t of fossil fuel fed into a burner per ton of fuel produced⁵. The RWGS reactor operates at 900 °C [3], while in the Fuel 1 plant it operates at “ca. 1000 °C” [2]. Furthermore, in the HTFT layout, the RWGS reactor is fed with hydrogen at high temperature. This is not the case in a LTFT layout, as PEM operates at 50°C to 90°C, compared to the 500 °C to 1000 °C of a SOEC electrolyser [56]. The exact operating temperature of the SOEC electrolyser employed in the Fuel 1 plant is unknown.

The other main processes employ the same main components, and differences in their operational parameters can be either quantified or are assumed to be identical.

The design of König et al. (2015) is modified for comparability, substituting the burner with electric heating [3]. With the designs being qualitatively equal, the specific amounts of materials per MJ of final product are assumed equal, and so are the impacts from the construction and EOL phases of the HTFT plant and LTFT plants (discussed in section 2.3). This section provides – in part – a qualitative description of the plant design section 2.3 is based upon, with regards to the validity of construction-phase impacts of the HTFT plant for the LTFT plants.

2.7.1. Electricity demand of the electric heater replacing the burner

The RWGS reactor in the original design of König et al. (2015) [3] requires 0.0443 MJ of thermal energy E_{th} per MJ of produced PtL-kerosene (based on [56]). In the model developed in this work, the burner it is replaced with an electric heater. Like in the model of König et al. (2015), the RWGS reactor is assumed to absorb heat through convection from process air. Given that the type of (electric) heater in the Fuel 1 plant is unknown, a likely heater technology is identified amongst commercially available options and literature.

⁵ According to Schmidt et al. (2019) [89] – who analyzed the work of König et al. (2015) [3] – in this configuration the burner emits 24 grams of CO₂ per MJ of SPK. For reference: CO₂ emissions from Jet A-1 combustion amount to 73.2 g CO₂/MJ [30].

A flanged heater is chosen, since it is suited for high temperature, low flow gas heating operation and offers a high electrical to thermal energy conversion efficiency [38,39]. Flanged heaters classify as direct resistance heaters (DRHs). Their electrical to thermal energy conversion efficiency $\eta_{el,th}$ is not disclosed by manufacturers such as Wattco (2020) [39] and is thus estimated with an engineering textbook discussing DRHs in detail [38]:

$$\eta_{el,th} = 90\%.$$

The electricity demand of the heater, E_{el} , is calculated as the ratio of E_{th} and the product of $\eta_{el,th}$ and the heat transfer efficiency between process air and the reactor, η_{HT} :

$$E_{el} = \frac{E_{th}}{\eta_{el,th}\eta_{HT}}.$$

The design of the flanged heater-RWGS reactor group determines η_{HT} , and is estimated based on the design of a RWGS reactor employed in laboratory tests conducted at temperatures of 875°C to 925°C [40], which are comparable with the operating temperatures of the RWGS reactors in this work. The disposition of the heating medium (process air) and heated medium (gases in the RWGS reactor) are as in a shell and tube heat exchanger. This can be appreciated comparing Figure S5 a) and b).

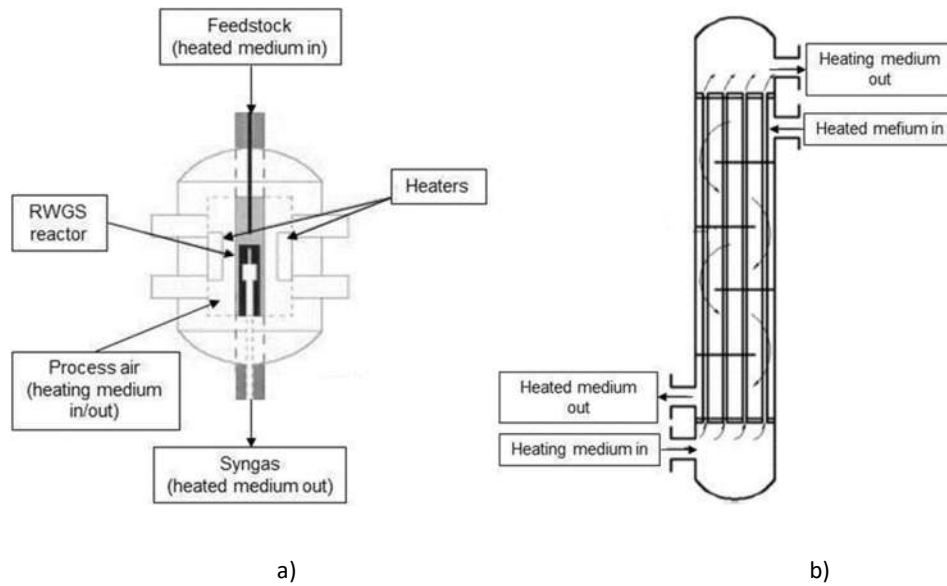


Figure S5. a) Schematic highlighting the disposition of the heating elements surrounding a RWGS reactor (based on [40]); b) Diagram of a typical shell and tube heat exchanger (based on [57])

In both designs, a flow of matter is concentric to, and in contact with, a substance at a higher temperature which is itself contained in a thermally isolated chamber. Based on the same observations made in section 2.6, and given the additional uncertainty due to a lack of design specifications, the efficiency of heat transfer is here conservatively assumed at 23%. For the given input gases (air, hydrogen and carbon dioxide), the calculated heat capacity ratio of the system amounts to $C_r = 0.42$ ⁶, which actually corresponds to a heat transfer efficiency of 56% [41]. Due to the high uncertainty concerning the design, applying a security factor of 2 to this estimate is considered an appropriate measure. Consequently:

$$\eta_{HT} = 23\%$$

and

$$E_{el} = 0.214 \left[\frac{MJ}{MJ, SPK} \right].$$

2.7.2. Effects on the main mass and energy flows due to the removal of the burner

In the plant design of König et al. (2015) [3] (hereafter referred to as “original design”), a fuel recycling unit (recycle splitter) redirects part of the hydrocarbons (2.8% of recycled portion of hydrocarbons) produced in refining to the aforementioned burner providing heat energy to the RWGS reactor (see Figure S6)⁷. The remaining 97.2% are recycled to the FT reactor (90.3%) and RWGS reactor (6.9%).

It is assumed that by eliminating the burner, the portion of recycled hydrocarbons originally fed into it can be redirected entirely to the internal recycle stream fed into the FT reactor. The effects of increasing the internal recycle stream are discussed below.

⁶ A more detailed description of this model goes beyond the scope of this work. For further details, the reader is invited to refer to Fakheri [41], which provided the theoretical background for estimating HT. The values needed to calculate the heat capacity ratio are the specific heat capacities of air, carbon dioxide and hydrogen (e.g. available from Gopal [90]) and the RWGS reactor feedstock's CO₂:H₂ ratio in weight (i.e. 16:1), which can be calculated knowing their stoichiometric ratios (i.e. 1:3 see Table S8) and atomic masses (H=1, C=12, O=16).

⁷ An additional 0.1t/h of fossil fuel is fed into the burner externally. This flow is removed from the original design alongside the burner.

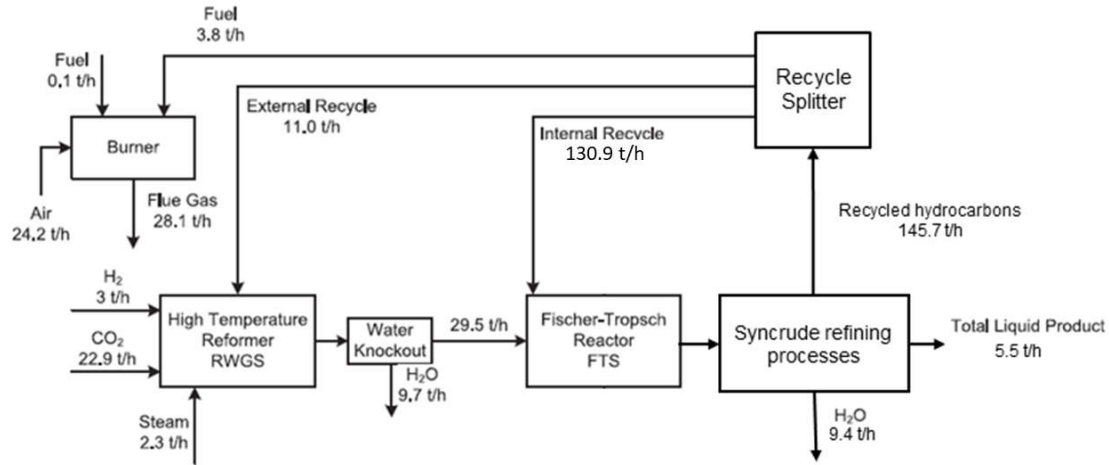


Figure S6. Original design of the LTFT plant (based on [3])

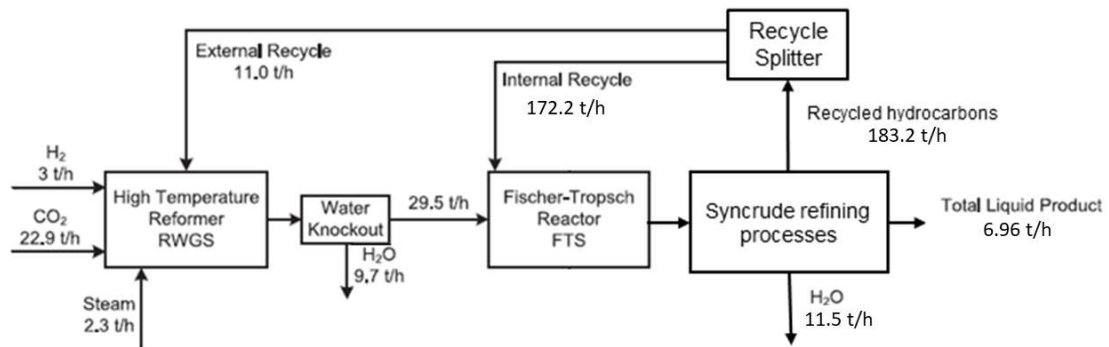


Figure S7. Modified design of the LTFT plant (based on [3])

Effect on mass flows

Out of the 3.9 t/h of fuel supplied to the burner in the original design, 3.8 t originate from the recycle splitter. From the recycle splitter, 130.9 t/h of recovered fuel are redirected to the FT reactor in the original design, along with 29.5 t/h from the RWGS reactor. At this mass input rate, the plant produces 5.5 t/h of liquid product.

In the adapted design, in a first iteration of the modified FTS-to-refining cycle, an increased quantity of 130.9 t/h + 3.8 t/h of fuel are redirected to the FT reactor. Supposing a linear relationship between input and output products, an increase by

$$\frac{3.8}{130.9 + 29.5} = 2.36 \%$$

of FT mass flow input causes the same percentual increase in liquid product output. In the first iteration ($i = 1$) of this process, the amount of produced fuel increases to

$$\text{Liquid products, modified design } (i = 1) = 5.5 \left[\frac{t}{h} \right] \cdot 1.0236 = 5.63 \left[\frac{t}{h} \right].$$

The increased mass flow input to the FT reactor causes an increase in the mass inflow of the recycle splitter, which in turn causes an increased input to the FT reactor. This feedback loop leads to an overall increase of the two output flows of the syncrude refining process (liquid hydrocarbons and water) which stabilizes after about 60 iterations. The mass flows in the modified design are displayed in Figure S7.

In the original design, the composition (w/w) of the output flows of the refining process are (see Figure S6):

Table S12. Composition of the output flows of the syncrude refining process by weight

Composition of the output flows of the syncrude refining process by weight			
Total (w/w)	Recycled hydrocarbons (to recycle splitter)	Water knockout	Liquid product
100%	90.85%	5.7%	3.45%

It is assumed that these shares remain constant. After 60 iterations of the modified FTS-to-refining cycle, the reaction stabilizes, and the output flows reach >99% of their asymptotic values.

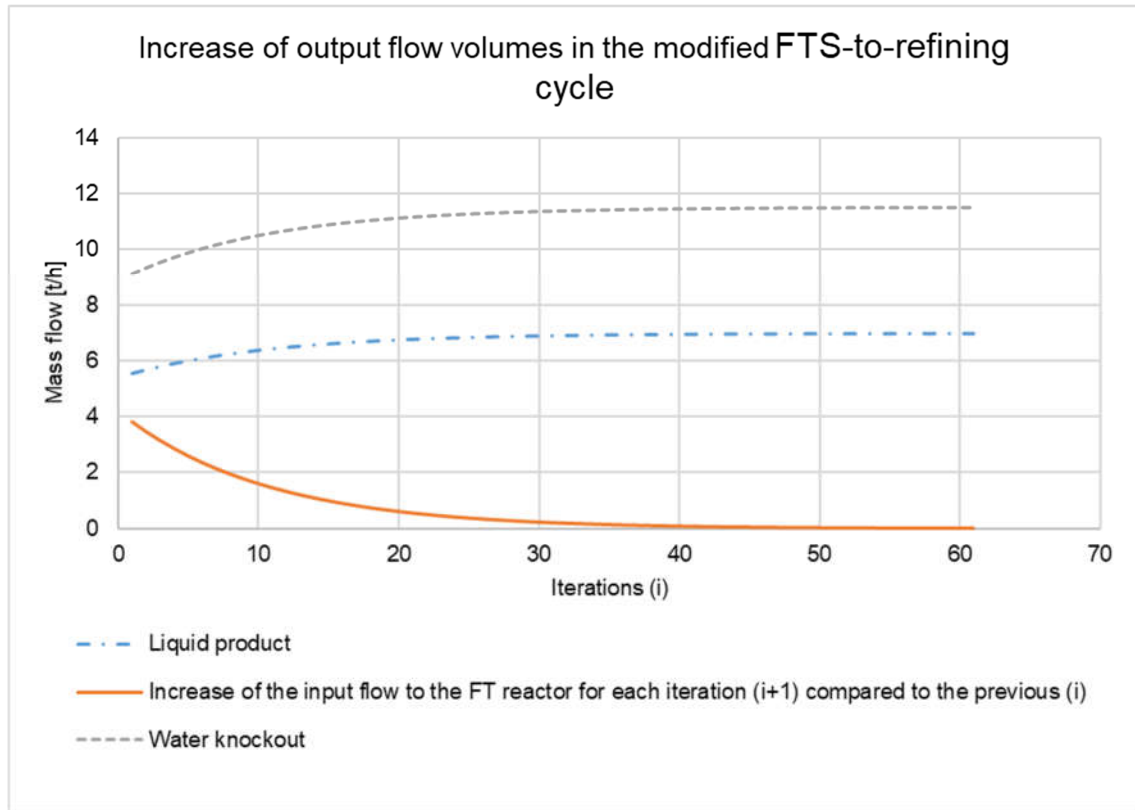


Figure S8. Increase of output flow volumes in the modified FTS-to-refining cycle

Absolute and relative increases are summarized in Figure S8 and Table S13.

Table S13. Increase of output flow volumes in the modified FTS-to-refining cycle compared to the original cycle

Increase of output flow volumes in the modified FTS-to-refining cycle compared to the original cycle		
Component	Water knockout [t/h]	Liquid product [t/h]
Original design	9.4	5.5
Modified design	11.5	6.96
Increase	25.8%	

Effect on excess heat energy ($E_{heat,new}$)

The input mass flow to the FT reactor increases too by 25.8%, and with it the total mass m of the produced syncrude. Since heat is a manifestation of kinetic energy ($E_{kin} = 0.5 \cdot mv^2$), assuming an

unchanged output velocity v of syncrude from the FT reactor, its kinetic energy increases by same amount.

In other words, the available amount of heat at a temperature of 225 °C from the FT reactor increases by 25.8%. The amount of heat power recovered from the FTS reaction ($P_{heat,FT}$) and from other sources⁸ ($P_{heat,other}$) in the original design, are extracted from König et al. (2015) [3]. In the modified design, the amount of heat $P_{heat,new}$ is:

$$P_{heat,new} = P_{heat,FT} \cdot 1.258 + P_{heat,other} = 21.86 \text{ MW} \cdot 1.258 + 3.84 \text{ MW} = 31.35 \text{ MW}$$

i.e.

$$E_{heat,new} = 0.367 \left[\frac{MJ}{MJ,SPK} \right]$$

in form of steam, out of which 0.043 MJ/MJ, PtL-kerosene are reused in the PtL-plant, resulting in a net amount of excess heat:

$$Excess \text{ heat, LTFT plants} = 0.323 \left[\frac{MJ}{MJ,SPK} \right].$$

For further details please refer to the original layout described by König et al. (2015) [3].

The electricity consumption of the main processes occurring in the LTFT plant are summarized in Table S14.

Table S14. Electricity consumption in the LTFT plant employing a PEM electrolyser by main process steps

Electricity consumption in the LTFT plant (PEM)						
Energy conversion efficiency	Total	Electrolysis	RWGS reactor	Compression	Refining	Unit
50.9%	1.963	1.759	0.169	0.033	0.002	$\left[\frac{MJ}{MJ,SPK} \right]$
Shares	100%	89.59%	8.59%	1.70%	0.12%	-

⁸ König et al. (2015) does not specify the origin of the other sources of waste heat. It is thus conservatively assumed that these are not affected by the redesign, which implies that their amount of excess heat remains unchanged in the modified design.

Since no fossil fuel is burned during PtL-kerosene production in the modified design, the direct emissions from the plant are reduced to zero⁹.

It can be expected that the discussed increase in flow volumes causes an increase in the energy consumption of refining processes. Since those consume only 0.12% of the final operational electricity (see Table S14), this effect is ignored.

2.7.3. Water consumption

Water consumption is discussed in 2.10.

2.8. DAC plant: impacts from construction and EOL

Table S15. Overview of the addressed objects, lifecycle phases and indicators in section 2.8.

Applies to	
Object(s):	DAC, Carbon Engineering and Climeworks plants
Lifecycle phase(s):	Construction and EOL
Indicator(s):	GWP, EP, AP, POCP, non-renewable primary energy, water consumption, land transformation

It is here described how impacts from the construction and EOL phases of the DAC plants are estimated. Following observations are based on literature.

Carbon Engineering refers to having conducted a LCA of its plant in one publication [17], but its extent is unclear and results only partially published.

2.8.1. GWP, EP, AP, POCP, and non-renewable primary energy

This section describes the approach to quantifying non-renewable primary energy, GWP, EP, AP and POCP.

From Lozanovski and Brandstetter (2015) [2] it can be concluded that impacts from construction and EOL of the Climeworks plant are negligible compared to the magnitudes of GWP, EP, AP, POCP, and

⁹ On the one hand, this is an approximation of a real system, because – as discussed in 2.3 – a flue gas torch is needed to ensure the safe operation of a distillation plant and is required by law. A flue gas torch causes direct emissions, yet those are assumed to be negligible, as discussed in 2.3 Therefore, the assumption for direct emissions to be zero is justified.

non-renewable primary energy of the HTFT plant in their study, since the impact share of the Climeworks DAC plant over its entire lifecycle **comprise <0.05% of any impact's magnitude of the product system.**

This is valid in the best-case scenario analyzed by Lozanovski and Brandstetter (2015) [2] (final electricity = 100% wind power and waste heat as final electricity sources). In scenarios where the final electricity is produced from fossil sources, the lifecycle impact share of the Climeworks DAC plant increases. This is attributable to the use-phase of the plant, where the impacts are caused indirectly by the electricity carriers.

The impacts from the construction and EOL phases of the Climeworks DAC plant are thus negligible.

One important technological and infrastructural difference between the Climeworks and Carbon Engineering DAC plants is that presence of a combined cycle gas turbine (CCGT) power plant within the Carbon Engineering plant. To take this difference into account, thereby increasing the comparability of the results for the two DAC plants, following approach is taken:

The impacts from the construction and EOL phases of the Carbon Engineering DAC plant, CCGT plant excluded, are assumed to be negligible. The impacts from construction, use and EOL of the CCGT plant are taken into account (see 2.9).

The latter assumption is assumed to have a negligible effect on the accuracy of results by analogy with the product system: the product system consumes high amounts of energy and water during operation, which are very likely to cause direct and indirect environmental impacts orders of magnitude higher than the contributions from the construction and EOL phases of the Carbon Engineering DAC plant.

2.8.2. Direct land transformation

Most recent direct land-use data for the Climeworks and Carbon Engineering DAC plants were summarized in August 2019 by Viebahn et al. (2019) [18] and serve as background data for this section.

Direct land-use from DAC can be defined as:

$$A_{direct} = A_{packings} + A_{facilities}$$

Where:

$$A_{packings} = \text{Area occupied by the } CO_2 \text{ capturing infrastructure}$$

$$A_{facilities} = \text{Area occupied by supporting facilities}$$

Carbon Engineering published land use data for $A_{packings}$ only, scaled on the average quantity of captured carbon dioxide per year:

$$A_{packings, Carbon Engineering} = 0.0016 \left[\frac{km^2}{Mt \frac{CO_2}{year}} \right]$$

However, Carbon Engineering concedes that actual land use would be significantly higher than the land use of packings alone [52].

Climeworks on the other hand provides a more comprehensive measure which includes packings and facilities for a total of:

$$A_{direct, Climeworks} = A_{packings, Climeworks} + A_{facilities, Climeworks} = 0.1 \left[\frac{km^2}{Mt \frac{CO_2}{year}} \right].$$

It is worth noting that this area mainly consists of clearance between facilities, according to an interview with Climeworks conducted by the authors of Viebahn et al. (2019) [18].

Due to a lack of data of the land use of facilities from the Carbon Engineering plant, direct land-use of the Carbon Engineering plant is conservatively assumed equal to direct land-use of the Climeworks plant.

$$A_{direct, Carbon Engineering} = A_{direct, Climeworks} = 0.1 \left[\frac{km^2}{Mt \frac{CO_2}{year}} \right].$$

As stated by Smith et al. (2016) [53], “[DAC plants] can be deployed on unproductive land that supplies few ecosystem services”. This study does not identify a specific location and aims at delivering

conservative estimates of the environmental impacts of the product system. Therefore, it is assumed that the quality of the used land is deteriorated indefinitely, and thus that it classifies as transformed land (i.e. land transformation A_{TR}) according to the LANCA definition [24].

A_{direct} is scaled according to the lifetime of the plants (20 years, according to Fasihi et al. (2019) [54]) and the quantity of feedstock CO₂ needed per unit PtL-kerosene (75g/MJ), and translated to land transformation (see Table S16).

Table S16. Direct land transformation from the Carbon Engineering and Climeworks DAC plants

Direct land transformation from the Carbon Engineering and Climeworks DAC plants	
$A_{TR\ direct, Carbon\ Engineering} = A_{TR\ direct, Climeworks}$	$3.75 \cdot 10^{-7} \left[\frac{m^2}{MJ, SPK} \right]$

This assumption is validated through an analysis of preliminary results. For all scenarios, direct land transformation from DAC plants contributes to <0.01% to overall land transformation (see 4.2.6.).

2.8.3. Indirect land transformation and water consumption

No data on indirect land transformation and water consumption from the construction and EOL phases of DAC plants were found in literature.

No inventory data to calculate those impacts were found (Ecoinvent 3.6, GaBi 2019, JRC and US federal LCA commons were searched), nor schematics of DAC plants were found, which could be used to compile an LCI.

It is assumed that indirect water consumption and land transformation attributable to both the Carbon Engineering and Climeworks DAC plant are negligible, since the product system consumes high amounts of energy and water during operation, which are very likely to cause direct and indirect environmental impacts orders of magnitude higher than the indirect contributions from DAC plants.

2.9. DAC plant: impacts from the use phase

Table S17. Overview of the addressed objects, lifecycle phase and indicators in section 2.9.

Applies to	
Object(s):	DAC – Carbon Engineering and Climeworks plants
Lifecycle phase(s):	Use phase
Indicator(s):	GWP, EP, AP, POCP, non-renewable primary energy, water consumption, land transformation

The two DAC plants studied in this work have direct and indirect impacts associated with their use-phase. An overview of the impact sources is provided in Table S18.

Table S18. Overview of impacts sources concerning the use phase of DAC plants

Overview of impacts sources concerning the use phase of DAC plants		
Manufacturer	Direct	Indirect
Climeworks	(none)	Electricity carriers
Carbon Engineering	Natural gas	Electricity carriers Natural gas and CCGT plant

The environmental impacts caused over the lifecycle of the energy carriers feeding into the DAC plants, as well as the associated non-renewable primary energy, land transformation and water consumption are ascribed to the use-phase of the DAC plants. These are here referred to as.

The electricity carriers include the entire lifecycle of the carriers' infrastructure. In order to increase the validity of a comparison with natural gas, the impacts from the infrastructure used to convert natural gas to electricity and heat in the Carbon Engineering DAC plant is taken into account (this is discussed further below).

Indirect impacts include the impacts from construction, use and EOL of the CCGT plant, and extraction and transport of natural gas. For consistency with the other energy carriers, those are ascribed to natural gas.

The Climeworks DAC plant does not cause any direct emissions and impacts during operation [58].

Indirect impacts are caused over the lifecycle of the electricity carriers powering the plant.

The Carbon Engineering DAC plant uses natural gas final energy carrier. Direct and indirect impacts are caused by the combustion of natural gas and related infrastructure.

Natural gas is converted to electricity and thermal energy in an on-site CCGT power plant with an operating power of 55.8 MW for an extraction capacity of 1 MtCO₂/year. The power plant provides 100% of the operational energy in the layout analyzed in this work. The consumption of natural gas amounts to 8.81 MJ/kgCO₂ captured [17]. The General Electric turbine GE LM 2500 DLE is here coupled with a heat recovery steam generator and a steam turbine. According to Carbon Engineering, this setup results in a thermal efficiency of 63.8% (electricity generated over LHV of natural gas) [17]¹⁰.

90% of CO₂ emissions from the gas turbine are scrubbed from the exhaust gases and captured [17]. The captured CO₂ is accounted for as (negative) captured atmospheric CO₂, while the turbine tailpipe emissions are accounted for as (positive) emissions to air.

2.9.1. GWP, EP, AP, POCP, non-renewable primary energy, land transformation, water consumption

The final energy carriers are natural gas (natural gas), and electricity from three sources (PV, wind power (Wind), and the German electricity mix (DE mix)) at different shares, adding up to 100% of final electricity consumption.

Each impact $I_{i,DAC}$ attributed to the use-phase of the DAC plants is calculated as the sum of the impacts I_{ij} of each energy carrier j . The impacts of the electricity carriers are weighted by their share s_j of the final electricity mix. The impacts of each energy carrier p are multiplied by the energy consumption E_{p,DAC_k} of a DAC plant in its layout k .

$$I_{i,DAC_k} \big|_{i,k=const} = \sum_{j,p} E_{p,DAC_k} \cdot I_{ij} \cdot s_j$$

$$I_{i,DAC_k} \big|_{i,k=const} = E_{el,DAC_k} (I_{i,PV} \cdot s_{PV} + I_{i,Wind} \cdot s_{Wind} + I_{i,DE mix} \cdot s_{DE mix}) + E_{NG,DAC_k} \cdot I_{i,NG}$$

¹⁰ This can be calculated from the flowchart in figure 2 of the cited work.

With the corresponding units:

$$\left[\frac{kg}{MJ, SPK} \right] = \left[\frac{MJ, el}{MJ, SPK} \right] \left[\frac{kg}{MJ, el} \right] + \left[\frac{MJ, NG}{MJ, SPK} \right] \left[\frac{kg}{MJ, NG} \right]$$

Where:

I_i	=	GWP, EP, AP, POCP, non-renewable primary energy, land transformation, water consumption.
j	=	PV, wind power, German electricity mix.
k	=	Climeworks DAC plant, Carbon Engineering DAC plant.
p	=	Electricity, natural gas.

Notably, the Climeworks plant condenses 1 ton of water from air per ton of captured CO₂ [18]¹¹, while the Carbon Engineering plant consumes 4.7 tons of water per ton of captured CO₂ [17].

2.9.2. Final energy consumption

In order to calculate the impacts concerning the use-phase of the DAC plants, their final energy consumption must be known. Values for final energy consumption of all plant designs are available in literature [17,18]. These are here scaled to the reference flow and summarized in Table S19 and Table S20.

When the Climeworks plant is coupled with the HTFT plant, enough excess heat is generated by the PtL-plant to supply the entire heat demand of the DAC plant of 0.54 MJ/MJ,PtL-kerosene. This is discussed in detail in 2.6.

However, when the Climeworks plant is coupled with a LTFT plant, only 0.323 MJ/MJ,PtL-kerosene of excess heat are available from the PtL-plant (discussed in 2.7). Under those circumstances, the Climeworks DAC plant is assumed to be equipped with an electric heater. This is discussed in section 2.9.

Consequently, when the Climeworks DAC plant is coupled with a LTFT PtL-plant, the heat demand from an external source decrease, since it is partially provided from within the plant itself. Therefore, a

¹¹ The authors do not specify the atmospheric conditions for which this rate is valid.

distinction is made between the final energy consumption of the Climeworks plant coupled with a HTFT PtL-plant, and LTFT PtL-plant (Table S20 and Table S21).

Table S19. Final energy consumption of the Carbon Engineering DAC plant

Final energy consumption of the Carbon Engineering DAC plant			
Type	Unit	Layout	
		95% Natural Gas + 5% Electricity	100% Natural Gas
Natural gas	$\left[\frac{MJ}{MJ, SPK} \right]$	0.394	0.661
Electricity	$\left[\frac{MJ}{MJ, SPK} \right]$	0.021	0
Total	$\left[\frac{MJ}{MJ, SPK} \right]$	0.415	0.661

Table S20. Final energy consumption of the Climeworks DAC plant when coupled with a HTFT PtL-plant

Final energy consumption of the Climeworks DAC plant – HTFT coupled			
Type	Unit	Layout	
		2019 plant type	Future plant type
Heat	$\left[\frac{MJ}{MJ, SPK} \right]$	0.540	0.405
Electricity	$\left[\frac{MJ}{MJ, SPK} \right]$	0.081	0.054
Total	$\left[\frac{MJ}{MJ, SPK} \right]$	0.621	0.459

Table S21. Final energy consumption of the Climeworks DAC plant when coupled with a LTFT PtL-plant

Final energy consumption of the Climeworks DAC plant – LTFT coupled			
Type	Unit	Layout	
		2019 plant type	Future plant type
Heat	$\left[\frac{MJ}{MJ, SPK} \right]$	0.323	0.323
Electricity	$\left[\frac{MJ}{MJ, SPK} \right]$	0.335	0.150
Total	$\left[\frac{MJ}{MJ, SPK} \right]$	0.658	0.473

2.9.3. Heat energy supply to the Climeworks plant coupled with the LTFT PtL-plant

It is assumed that the remaining heat demand ΔE_{th} is covered by an electric counterflow heat exchanger. The efficiency of heat transfer η_{th} is estimated at 95% based on a heat capacity ratio estimate of $C_r = 0.8$ [41]:

$$\eta_{th} = 95\%.$$

The heating fluid is assumed to be heated by DRH, with a thermal energy conversion efficiency $\eta_{el,th}$ of 90% [38]:

$$\eta_{el,th} = 90\%.$$

The resulting additional final electricity demand $E_{el,ADD}$ can thus be calculated as:

$$E_{el,ADD} = 0.9 \cdot 0.95 \cdot \Delta E_{th}.$$

The amounts of ΔE_{th} and $E_{el,ADD}$ are summarized in

Table S22.

Table S22. Additional final electricity demand of the Climeworks DAC plant when coupled with a LTFT PtL-plant

Additional final electricity demand of the Climeworks DAC plant – LTFT coupled
--

Type	Unit	Layout	
		2019 plant type	Future plant type
ΔE_{th}	$\left[\frac{MJ}{MJ, SPK} \right]$	0.217	0.082
$E_{el,ADD}$	$\left[\frac{MJ}{MJ, SPK} \right]$	0.254	0.096

Impacts from the infrastructure needed for the additional heat supply are assumed negligible by analogy with the considerations on the heat exchanger in the HTFT plant presented in 2.3.1.

2.9.4. Natural gas: GWP, EP, AP, and POCP

GWP, EP, AP, and POCP of natural gas consumed at the CCGT plant within the Carbon Engineering DAC plant are calculated by scaling the lifecycle environmental impacts of natural gas consumed at a utility scale 300 MW CCGT plant. The plant operates in Germany, the reference year of the study is 2010 (even though the study was published 2006). The system boundary is comparable to the boundary in the present work as it includes impacts from construction, use and EOL of the CCGT plant [16].

LCIA results for the CCGT plant are scaled based on the ratio of the energy conversion efficiency of the plant from literature (50%) and of the Carbon Engineering CCGT plant (63.8% [17]).

$$\text{Scaling factor, CCGT at DAC} = \frac{50}{63.8} = 0.78.$$

2.9.5. Natural gas: non-renewable primary energy and land transformation

Non-renewable primary energy is calculated with a “[non-renewable] primary energy factor” of 1.1 MJ per MJ of natural gas used in EU norms applied in several European regions, including Germany, according to Schüwer et al. (2015) [15].

$$\text{Primary energy factor} = 1.1 \left[\frac{MJ}{MJ} \right].$$

2.9.6. Note on indirect land transformation and water consumption

The amount of **indirect land transformation and water consumption** associated with the **electricity carriers** used during operation is described in the sections on electricity from wind power, PV and the German electricity mix.

The value for **indirect land transformation** from **natural gas** is calculated as upstream land transformation from natural gas extraction (in Germany with reference year 2015). It is obtained from correspondence with Sphera, per unit of electricity produced at natural gas power plants [14] and amounts to 0.000102 m²/MJ, electricity in line with literature, the average thermal efficiency of natural gas-fired power plants in Germany can be assumed at 50%, which translates to:

$$\text{Indirect land transformation, natural gas} = 0.000051 \left[\frac{\text{m}^2}{\text{MJ, NG}} \right].$$

Water consumption from natural gas extraction and transport is negligible at 3.6 ml per MJ delivered to the plant (estimated from Mielke et al. (2010) [59])¹².

No water is consumed directly during the use-phase of the DAC plants [17,58].

2.10 Product system: water consumption

Table S23. Overview of the addressed objects, lifecycle phases and indicators in section 2.10

Applies to	
Object(s):	Product system
Lifecycle phase(s):	Entire lifecycle
Indicator(s):	Water consumption

Water is consumed directly and indirectly in the product system. A significant amount of water is consumed during the use phase of the PtL-kerosene production plant by water electrolysis (i.e., direct water consumption) and by the Carbon Engineering DAC plant (*H₂O*, *Carbon Engineering*). Water is

¹² i.e. 1 gallon per MMBtu. This is an average value valid for natural gas in the United States. It is assumed that the same order of magnitude is valid for natural gas consumed in Germany. Given the amount of direct water consumption, which is several orders of magnitude greater, this amount is negligible.

further produced as a side product in the PtL-plant, and is condensed from air by the Climeworks DAC plant.

Water is further consumed indirectly by the background system.

2.10.1. Direct consumption from electrolysis

The electrolyzers consume deionized water during operation. Water, sourced as freshwater, is treated in a deionizer operating at a water conversion efficiency $\eta_{deionizer}$ of 99% (after Anderson et al. (2010) [43]):

$$\eta_{deionizer} = 99\%.$$

The deionized water consumption per kg of hydrogen of the electrolyzers (H_2O_{IN}) is summarized in Table S24.

Table S24. Deionized water consumption by type of electrolyser

Deionized water consumption by type of electrolyser		
Electrolyser	Rate of consumption [kg/kgH ₂]	Reference
SOEC	9.1	[44]
PEM	18.04	[44]

2.10.2. On-site water production: water as a side product of the PtL-plant

In the PtL-plant, all processes downstream of the RWGS reaction produce a significant amount of water as side product, which is extracted from the process flows with scrubbers¹³. The water is then purified and reused as input to the electrolyser¹⁴. As discussed in previous sections, for both HTFT and LTFT plants, the main plant components between the point of hydrogen production (electrolyser output)

¹³ devices used to purify streams of hydrocarbons from undesired side products.

¹⁴ While water is not recycled to the electrolyser both in the LTFT plant in the design of König et al. (2015), nor in the Fuel 1 plant, it is technically feasible as mentioned by Fasihi et al. (2016) [36].

and refinery output are identical (exception made for auxiliary components such as heat recovery units).

It is assumed that the amount of water knockout is the same for both HTFT and LTFT plants.

The energy specific water knockout is calculated from the values summarized in Table S13. Considering that the LHVs of all fuels produced in the LTFT plant deviate from one another by <0.1% (from the power and mass flows in König et al. (2015) [3]), from an energy standpoint, the liquid product can be treated as if it was composed by PtL-kerosene alone. Consequentially, the scrubbed water per MJ of PtL-kerosene is:

$$H_2O_{out} = -\frac{11.5 \left[\frac{t, H_2O}{h} \right]}{6.96 \left[\frac{t, SPK}{h} \right] \cdot LHV, SPK} = -0.037 \left[\frac{kg}{MJ, SPK} \right].$$

Among the studied literature, one work mentions the possibility of reusing scrubbed water, but does not specify to which extent it can be recovered [36].

It is here assumed that 90% of the knocked-out water is reused as an input to the electrolyser, after having been purified and deionized. This can be described as water reuse efficiency:

$$\eta_{water\ reuse} = 90\%.$$

2.10.3. On-site water production: water as a side product of DAC

In the Climeworks layout, water is obtained as a side product of the extraction process of carbon dioxide from air and amounts to 1 ton of water per ton of CO₂ [18]. The authors do not specify under which climatic conditions this is the case. Considering the amount of carbon dioxide needed per unit of PtL-kerosene (discussed in 2.2.):

$$H_2O_{out, Climeworks} = -0.075 \left[\frac{kg}{MJ, SPK} \right].$$

$H_2O_{OUT, Climeworks}$ is assumed to be constant.

2.10.4. Total direct water consumption

Combining the above, direct water consumption H_2O_{TOT} is calculated as:

$$H_2O_{tot} = \frac{H_2O_{in}}{\eta_{deionizer}} + H_2O_{Carbon Engineering} + H_2O_{out} \cdot \eta_{water reuse}$$

and as

$$H_2O_{tot} = \frac{H_2O_{in}}{\eta_{deionizer}} + (H_2O_{out} + H_2O_{out, cw}) \cdot \eta_{water reuse}$$

if the Climeworks DAC plant is employed.

2.10.5. Indirect and total water consumption

Water is consumed indirectly over the lifecycle of the final electricity sources. Total water consumption is the sum of direct and indirect water consumption.

2.11. Electricity from PV

Table S25. Overview of the addressed objects, lifecycle phases and indicators in section 2.11.

Applies to	
Object(s):	Electricity from PV
Lifecycle phase(s):	Entire lifecycle
Indicator(s):	GWP, EP, AP, POCP, non-renewable primary energy, water consumption, land transformation

The environmental impacts from the panels are here quantified for Germany in 2015 based on a lifecycle analysis of poly-crystalline PV modules produced in China in 2014, based on data for “typical PV companies in China” [13]. The panels are arranged in a flat plate array without tracking mechanisms, because this is the most common PV array design in use today, along with flat plate arrays with tilt adjustment, according to US department of energy [12]. The former layout is chosen, as it represents the more conservative option, having a lower specific energy yield.

In Fu et al. (2014) [13], the impacts are quantified per unit energy delivered to the electricity grid, given a solar irradiation of $1,300 \left[\frac{kWh}{m^2 a} \right]$. The environmental impacts per kWh of electricity generated by PV

systems is thus a function of their life-cycle energy generation capacity, which is a function of solar irradiation.

The authors do not specify the type of solar irradiation used in their calculations. As GHI is commonly used for PV system sizing¹⁵, it is assumed that the authors have used this metric.

2.12. Electricity from wind power

Table S26. Overview of the addressed object, lifecycle phases and indicators in section 2.12.

Applies to	
Object(s):	Electricity from wind power
Lifecycle phase(s):	Entire lifecycle
Indicator(s):	GWP, EP, AP, POCP, non-renewable primary energy, water consumption, land transformation

The calculations of the environmental impacts associated with electricity from wind power are here laid out.

2.12.1. GWP, EP, AP, POCP, non-renewable primary energy and water consumption

Values of GWP, EP, AP, POCP, water consumption and non-renewable primary energy are adapted from a lifecycle analysis of a 50 MW onshore wind farm employing 2 MW wind turbines manufactured by Vestas [7]. The functional unit of the study is the production of 1 kWh of electricity delivered to the electricity grid from a 50 MW virtual wind park composed by 25 2MW Vestas Wind turbines. The functional unit is thus compatible with the setup of the product system in this work, where the electricity is directly fed into the product system.

The energy-specific impacts identified in the study are here scaled according to the amount of energy produced at the geographical location of the product system, i.e., with the ratio of the capacity factors.

The capacity factor c of a wind turbine (or wind farm) is the ratio of the output electrical energy E_{el} over a given amount of time and the theoretically maximum energy output over the same period, thus with the turbine operating at nominal power P_N . This value is typically calculated per annum.

¹⁵ Based on own experience in the field.

$$c_{wind} = \frac{E_{el} \left[\frac{MWh}{a} \right]}{P_N [MW] 365.25 \left[\frac{d}{a} \right] 24 \left[\frac{h}{d} \right]}$$

The capacity factor used by Vestas is (based on [7]):

$$c_{Vestas} = 0.432.$$

The capacity factor for a plant operating in Germany in 2015 is calculated based on the total onshore nominal wind power installed nationwide in 2015 and the total generation from onshore wind turbines in the same year (based on [11]):

$$c_{Wind DE 2015} = 0.206.$$

In both cases, the lifetime of the wind turbines is assumed to be 20 years in line with Razdan and Garrett (2015) [7].

The ratio of the capacity factors (or: scaling factor) $f_{c,wind}$ is:

$$Scaling\ factor, wind\ power = f_{c,wind} = \frac{c_{Vestas}}{c_{Wind DE 2015}} = 2.092.$$

2.12.2. Direct land transformation

Quantifying the amount of area undergoing changes due to the installation of wind turbines is not trivial. This amount varies by one or two order of magnitudes across studies, engineering manuals and reports, depending on the definition of the terms used to measure land-use quantities such as “occupied land”, “land use”, “permanently occupied land”, and so on, which are not defined univocally across literature [66–69].

The most comprehensive work providing clarity on the topic is a 2009 report by the US National Renewable Energy Laboratory (NREL) on “land use requirements” of wind farms in the US [67]. The work quantifies the differences in quantity and characteristics of area occupied and/or transformed by different wind farms. It is based on 172 existing or proposed projects as of 2009 in the U.S., with a cumulative nominal capacity of more than 26 GW. The study additionally analyzes the wording used in

several thematically relevant studies and translates it into two land-use metrics relevant for wind farms:

- (a) **Direct impact area**, i.e. “disturbed land due to physical infrastructure development”, divided in permanent and temporary direct impact area [67].

Under the conservative assumption that the transformed land is transformed indefinitely, and that it was of higher quality before the installation of a wind power related infrastructure, permanent direct impact area is positive land transformation as defined by Sphera [24]. This is a conservative assumption, as the change in the quality of land can be expected to be different from project to project, implying that land quality is not necessarily degraded.

- (b) **Total area**, i.e. “land associated with the complete wind plant project” [67]. Figure S9 illustrates both definitions. Infrastructure contributing to land transformation is labelled as “permanent”.

The cited study finds that “there is substantial variation among the reported area requirements [...]. For the permanent direct impact, the range is about 0.06 hectares/MW to about 2.4 hectares/MW; however, approximately 80% of the projects (both number of projects and total capacity) report direct land use at below 0.4 hectares/MW.” [67], see Figure S10.

The average nominal power of the wind turbines in the study is 1.6 MW [67]. Nominal power per wind turbine of at least 2 MW were the norm from 2015 onward in Germany [70]. Direct impact area depends on the number of turbines needed to produce a given amount of power (as can be for example concluded from Figure S9). It follows that the direct impact area of wind turbines in Germany is lower than the average found in the cited study.

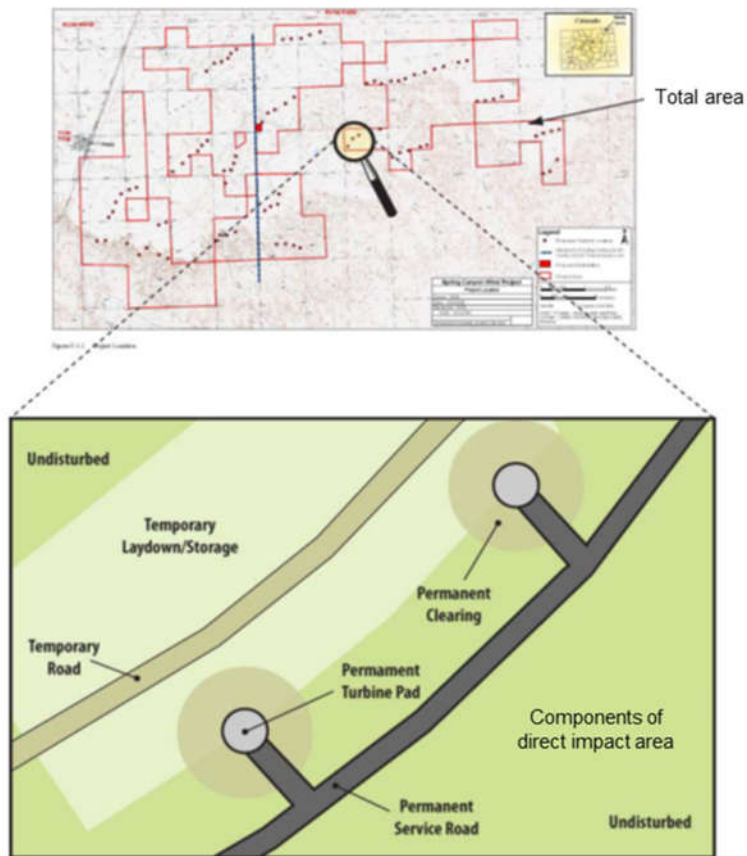


Figure S9. Visual description of total area and direct impact area resulting from wind power infrastructure (adapted from Denholm et al. (2009) [67])¹⁶

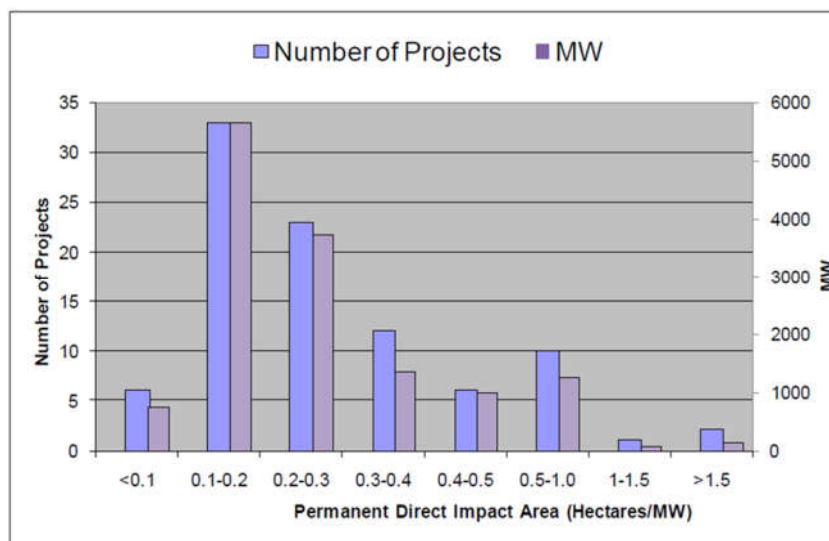


Figure S10. Permanent direct impact area of onshore wind farms (from Denholm et al. (2009) [67])

¹⁶ This illustration is not meant to represent any specific project and the actual components and configuration of direct impact area vary among projects.

Permanent direct impact area:

Considering the above, the permanent direct impact area (i.e., direct land transformation) is here calculated as the mean of the values < 0.4 ha/MW, corresponding to 80% of the studied power capacity. It amounts to 0.25 ha/MW. This choice is considered a measured trade off. On the one hand, by excluding the extremes, values that are likely to be less representative for the 2 MW wind turbines (part of the product system under study) are excluded. On the other hand, a high percentage of the sample from the study is considered.

Factoring in the capacity factor and lifetime of a wind turbine, land transformation amounts to:

$$\text{Land transformation} \left[\frac{m^2}{MJ} \right] = \frac{\frac{\text{Direct impact area} \left[\frac{m^2}{MW} \right]}{P_N}}{c \cdot 8,760 \left[\frac{h}{a} \right] \cdot \text{lifetime} [a] \cdot 10^3 \cdot 3.6}$$

Using the average capacity factor for Germany in 2015, and assuming a lifetime of 20 years (in accordance to Razdan and Garrett (2015) [7]), land transformation amounts to:

$$\text{Land transformation, wind power, direct} = 1.90 \cdot 10^{-5} \left[\frac{m^2}{MJ} \right].$$

Total area:

Unlike for the other components of the product system, it is found useful to quantify the total area associated with electricity from wind power, the main reason being that it resides at the center of current public debate surrounding wind power, which makes it interesting for the intended recipients of this work [71]. It is pointed out that out of the total area, only a fraction classifies as land transformation, while the rest is unchanged.

The total area is calculated based on a report from the German Ministry for Environment (UBA), which estimates the total amount of area available in Germany for installing onshore wind power at 49,361 km², and the total wind power installations possible on that area resulting in 1,187.84 GW of nominal power. In the report, a capacity factor of $c_{UBA} = 0.278$ is used. At the given capacity factor, the total area according to the UBA study amounts to

$$Total\ area,\ wind\ power,\ UBA = 4.73 \cdot 10^{-3} \left[\frac{m^2}{MJ} \right].$$

This value is scaled on the wind conditions in Germany in 2015 with the ratio of the capacity factors and amounts to:

$$Total\ area,\ wind\ power = Total\ area,\ wind\ power,\ UBA \frac{c_{UBA}}{c_{Wind\ DE\ 2015}}$$

$$Total\ area,\ wind\ power = 6.38 \cdot 10^{-3} \left[\frac{m^2}{MJ} \right].$$

It is noted that offshore wind power is excluded from this analysis. The main reason being that the modeled PtL-plants are assumed to operate off-grid, on land¹⁷.

2.12.3. Indirect land transformation

A significant amount of land transformation is caused by upstream activities related to wind power plants operating in Germany. This amount is provided by Sphera and is based on the LANCA method for the evaluation of land quantities. The other data on wind power used for the calculations herein is itself valid for Germany in 2015 and its impacts are computed with the same LCIA method as for indirect land transformation. On the other hand, the value below is valid for the mix of wind farms in Germany with reference year 2015, out of which only 24% were produced by Vestas [6].

$$Land\ Transformation,\ wind\ power,\ indirect = 1.46 \cdot 10^{-4} \left[\frac{m^2}{MJ} \right].$$

¹⁷ For completeness it is noted that offshore wind power constitutes only about 2.7% of globally installed wind power capacity [91,92]. Including figures for offshore wind power would decrease energy specific area needs, as offshore wind power has capacity factors higher than onshore wind [93].

2.13. Electricity from the German electricity mix

Table S27. Overview of the addressed object, lifecycle phases and indicators in section 2.13.

Applies to	
Object(s):	Electricity from the German electricity mix
Lifecycle phase(s):	Entire lifecycle
Indicator(s):	GWP, EP, AP, POCP, non-renewable primary energy, water consumption, land transformation

LCIA results for electricity from the German electricity mix are calculated in GaBi ts, version 9 (demo version) and are based on the 2019 GaBi database.

Land transformation is obtained from the 2020 GaBi database through correspondence with Sphera. This choice is made, because Sphera updated their methodology for land-use quantities to deliver more accurate results recently, making older methodologies and data such as in the GaBi ts demo version obsolete.

2.14. PtL-kerosene: impacts

Table S28. Overview of the addressed object, lifecycle phases and indicators in section 2.14.

Applies to	
Object(s):	PtL-kerosene
Lifecycle phase(s):	Whole lifecycle
Indicator(s):	GWP, EP, AP, POCP, non-renewable primary energy, water consumption, and land transformation

The impacts from each component of the product system are expressed over 1 MJ of produced PtL-kerosene.

2.14.1. Production

The impacts from the production of PtL-kerosene are thus the sum of the impacts of each process or flow of the product system.

2.14.2. Combustion

The combustion emissions profiles (or: emissions profiles) of Jet A-1 and PtL-kerosene present some differences which influence the magnitude of the environmental impacts resulting from the fuels' combustion. Additionally, the chemical composition (and thus the emissions profile and subsequent

environmental impacts) of PtL-kerosene varies slightly with respect to different feedstock sources and production methods [19,72]. It is thus stressed out that here “PtL-kerosene” is understood to be produced via FTS. It is also noted that the emissions profile of FT-PtL-kerosene produced from CO₂ and hydrogen as feedstock has not been characterized at the time of the literature review, but that it is assumed to be identical to the emissions profile of FT-PtL-kerosene produced from a different kind of feedstock.

The emissions profile of PtL-kerosene has lower contents of certain characterization factors¹⁸ of AP and EP. Knowing the AP and EP values from the combustion of (1 MJ of) Jet A-1, and the differences between the combustion products of the two, the values for AP and EP for PtL-kerosene are calculated. The differences in the combustion profiles do not affect GWP-100 nor POCP.

Acidification due to Jet A-1 combustion is caused by SO₂ (12%) and NO_x (88%) [14]. In FT PtL-kerosene, tailpipe SO₂ emissions are absent (100% reduction) and NO_x emissions are 8% lower compared to Jet A-1 [19–21]. As a result, AP from PtL-kerosene combustion is 18.9% lower.

Eutrophication due to Jet A-1 combustion is caused by NO_x (99%) [14]. Since tailpipe NO_x emissions are 8% lower in FT PtL-kerosene, the EP of PtL-kerosene is 7.9% lower.

Additionally, considering that the gravimetric energy density of Jet A-1 (43.2 MJ/kg) is 2.5% lower than in PtL-kerosene (44.1 MJ/kg), the emissions per unit energy are 2.5% lower in PtL-kerosene (based on Elgowainy et al. (2012) [26]).

Considering that both fuels are used under the same conditions, the equations below describe the cited environmental impacts of PtL-kerosene combustion ($i_{SPK,TTWa}$) – indicated by the *TtWa* subscript – as a function of the environmental impacts of Jet A-1 combustion ($i_{Jet A-1,TTWa}$). The relative contributions of the characterization factors to the impacts are defined in the LCIA methodology used in this work (CML 2001, April 2016 version, [73,74]).

¹⁸ i.e. a substance which contributes to an environmental impact.

$$GWP_{SPK,TTWa} = 0.975 \cdot GWP_{JetA1,TtWa}$$

$$AP_{SPK,TTWa} = 0 + 0.975 \cdot 0.88 \cdot 0.92 \cdot AP_{JetA1,TtWa}$$

$$EP_{SPK,TTWa} = 0.975 \cdot 0.99 \cdot 0.92 \cdot EP_{JetA1,TtWa}$$

$$POCP_{SPK,TTWa} = 0.975 \cdot POCP_{JetA1,TtWa}$$

2.15. Jet A-1: impacts

Table S29. Overview of the addressed object, lifecycle phases and indicators in section 2.15.

Applies to	
Object(s):	Jet A-1
Lifecycle phase(s):	Entire lifecycle
Indicator(s):	GWP, EP, AP, POCP, non-renewable primary energy, water consumption, land transformation

LCIA results for Jet A-1 produced in Germany are calculated in GaBi ts, version 9 (demo version) and are based on the 2019 GaBi database.

Land transformation is obtained from the 2020 GaBi database through correspondence with Sphera. This choice is made, because Sphera updated their methodology for land-use quantities to deliver more accurate results recently, making older methodologies and data such as in the GaBi ts demo version obsolete.

2.16. Jet A-1: effects of renewable electricity on environmental impacts

Table S30. Overview of the addressed object, lifecycle phases and indicators in section 2.16.

Applies to	
Object(s):	Jet A-1
Lifecycle phase(s):	Entire lifecycle
Indicator(s):	GWP, EP, AP, POCP, non-renewable primary energy, water consumption, land transformation

In order to deliver an accurate comparative analysis of PtL-kerosene and Jet A-1, it is useful to explore how the impacts of Jet A-1 are influenced if the same final electricity mix deployed to the product system is used in its production.

To do so, first, the amount of electricity consumed in fuel production is quantified, as well as the primary energy required over the fuel's lifecycle. According to [14], 84% of primary energy from Jet A-1 is embedded (fossil) chemical energy, while the remaining 16% is required for fuel production.

According to European Commission [75], 10% of the production energy in refineries is, on average, electrical¹⁹, the rest mainly being chemical energy from petrol or other fossil energy carriers. The electricity is commonly produced on-site from (fossil) refinery by-products, with some cases where electricity is bought from a utility [75]. Consequently, a maximum of 1.6% of primary energy is delivered as electricity and can potentially be renewable.

Even if this share of primary energy was completely renewable, the environmental impacts would be dominated by the combustion of fossil energy carriers, or – in production – by their use and the use of affiliated infrastructure and production practices.

It is thus concluded that the environmental impacts of Jet A-1 are constant, independently of the final electricity mix.

2.17. Global aviation: tailpipe emissions share of stratospheric CO₂

The fuels studied in this work are combusted in an aircraft operating on a flight path representing the global average flight path for commercial aviation. The characteristics of the flight path are relevant to calculate the RFI.

Specifically, in order to calculate the RFI, the share of CO₂ emissions from the aircraft occurring in the stratosphere, i.e., the CCD (climb, cruise, descent) cycle, must be known (see Figure S11; LTO=landing and take-off).

¹⁹ This value was calculated in 2015 by the European Joint Research Center in their Best Available Techniques (BAT) Reference Document for the refining of mineral oil and gas and is based upon estimated primary energy consumption for refineries in the US.

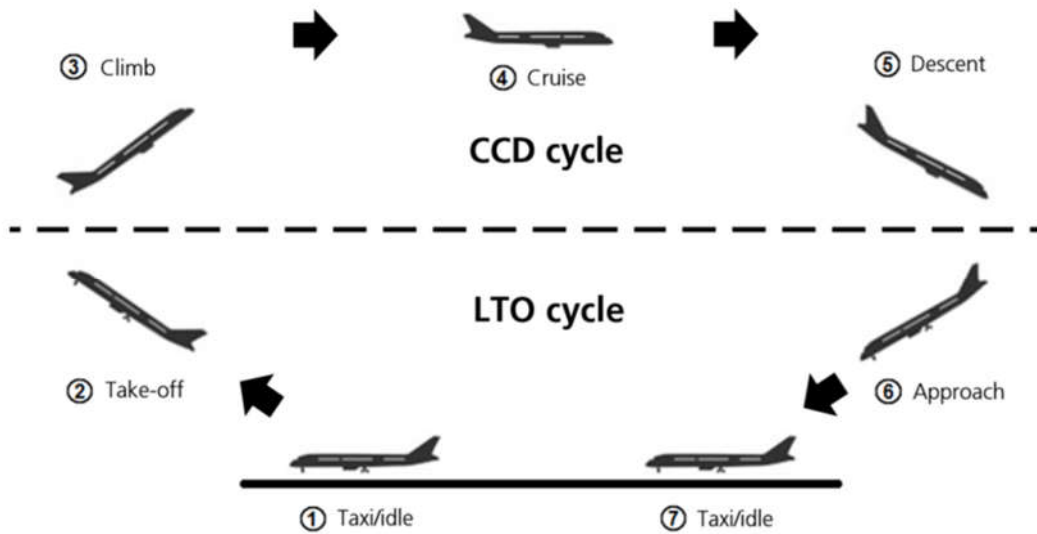


Figure S11. Schematic of a commercial flight cycle (from Defilippi [76])

The share of stratospheric CO₂ emissions is equal to the share of fuel consumption during the CCD cycle. The latter is calculated from data for fuel consumption volumes from commercial aviation in the US in 2009. Comprising a total of 7.9 million flights, fuel consumption amounted to 43.9 million tons [26] or 22% of global commercial aviation fuel consumption (i.e. 201 million tons [77]).

It is assumed that the data collected by Elgowainy et al. (2012) [26] are representative of global average flight paths and thus valid for this work. The data is evaluated in MS Excel. The LTO share of fuel combustion, and thus the share of stratospheric CO₂ amount to:

$$\text{Share stratospheric CO}_2 = 91.1\%.$$

2.18. Water purifier and deionizer

A water purifier and deionizer are considered in the product system in order to calculate the amount of water consumption of the product system more accurately. However, the environmental impacts caused over the lifecycle of those components are not included in this work.

In general, water can be for example purified through reverse osmosis [78] or other techniques, all of which consume a relatively negligible amount of electricity compared to the electrolysis process [78].

Regardless of the water filtration and deionization technique, approx. 0.12 kWh/m³ to 1 kWh/m³, i.e.

0.00012 kWh/l to 0.001 kWh/l are consumed for a concentration of ions in the water to be treated equivalent to brackish water²⁰ [43].

In this work, freshwater is assumed to be fed into the filtration and deionization system. Therefore, an electricity consumption < 0.001 kWh/l can be expected. Among the studied product system layouts, the highest rate of water consumption is 0.4 l/MJ of PtL-kerosene, implying a maximum electricity consumption of $0.001 \text{ kWh/l} \cdot 0.4 \text{ l/MJ} = 0.0004 \text{ kWh/MJ}$ of PtL-kerosene. This amount is negligible, compared to an electricity consumption of 1.304 MJ/MJ PtL-kerosene in the product system layout requiring the lowest amount of electricity among the studied layouts and so are the associated environmental impacts.

The environmental impacts associated with construction, EOL and maintenance cannot be generalized, since different filtration and deionization techniques require different types and amounts of resources [43,78]. However, considering the size of the product system and the fact that despite its size, most impacts shares arise during operation (see 4.1.), it is assumed that construction, EOL and maintenance of water filtration and deionization have a negligible effect on the overall environmental impacts of PtL-kerosene.

2.19. Comparability of LCIA methods

The LCIA methods used to classify and characterize elementary flows are addressed in this section, along with key methodological choices on data gathering and evaluation.

The environmental impact indicators GWP, EP, AP and POCP are calculated with the CML 2001 method, version 2015 or equivalent.

The environmental impacts of some processes or flows are calculated as combining LCIA results from literature, which are all calculated with different versions of the CML 2001 method. The differences between the versions (2007, 2013, 2014 and 2015) are investigated (CML version history available at

²⁰ i.e. a mixture of sea- and freshwater. As such, it has a higher concentration of ions than freshwater. The ionic concentration is the main driver of electricity consumption [43].

[73]). They do not affect the calculation methods of the indicators studied in this work. All the LCIA results from literature are based on LCAs adopting a cradle-to-grave boundary. Considered the above, the use of impact assessment values from literature calculated with the different CML versions is justified. An overview of the LCIA methods and annexed inventory data types (used in the references) for the foreground and background systems are summarized in

Table S31. Referenced sources either rely on primary data, on secondary data from literature.

In some cases, the LCIA results are adjusted in order to adapt them to the studied processes. For example, the environmental impacts from PtL-kerosene combustion are calculated based on the quantification of the difference between elementary flows of fossil Jet A-1 and PtL-kerosene.

Table S31. Overview of the sources used to quantify GWP, AP, EP and POCP, and of the type of inventory data and LCIA methods used in the sources, by process or flow

Overview of the sources used to quantify GWP, AP, EP and POCP, and of the type of inventory data and LCIA methods used in the sources, by process or flow			
Process or flow	LCIA methods, version	Inventory data type	Reference
HTFT plant (construction, EOL)	CML 2001, 2014	primary (I)	[2]
LTFT plant (construction, EOL)	CML 2001, 2014	primary (I)	[2]
DAC plant (construction, EOL)	(contribution unknown at the time of the literature review/undisclosed), qualitative assessment based on CML 2001, 2014	primary (exp)	based on [2]
PtL-kerosene production plant (operation)	CML 2001, 2015	primary (exp) secondary (I)	[3,17,18]
Natural Gas (entire lifecycle)	CML 2001, 2014; ReCiPe, 2008 (EP)	primary (I)	[15,68]
El. from PV (entire lifecycle)	CML 2001, 2007	primary (I) GaBi db, 2020	[13,14,78]
El. from wind power (entire lifecycle)	CML 2001, 2013	primary (I) GaBi db, 2020	[7,14]
El. from German el. mix (entire lifecycle)	CML 2001, 2015	GaBi db, 2019 GaBi db, 2020	[14]
Jet A-1 (entire lifecycle)	CML 2001, 2015	GaBi db, 2019 GaBi db, 2020	[14]
PtL-kerosene (combustion)	CML 2001, 2015	secondary (I) GaBi db, 2019	[14,20,21]

(I) = from literature; El. = Electricity

2.20. Jet fuel

Based on fuel consumption data reported by International Energy Agency [80] it can be concluded that >99.5% (w/w) of aviation fuel consumed worldwide is either Jet A or Jet A-1

3. Overview of main assumptions and parameters

Table S32. Overview of main assumptions and parameters

Item	Value	Unit	Notes	Reference
Physical properties				
Jet A-1 heat of combustion (LHV)	43.2	[MJ/kg]		[26]
Jet A-1 gravimetric density at 15°C	0.8	[kg/l]		[81]
Hydrogen heat of combustion (LHV)	120	[MJ/kg]		[82]
E-PtL-kerosene heat of combustion (LHV)	44.1	[MJ/kg]		[26]
E-PtL-kerosene gravimetric density at 15°C	0.75	[kg/l]		[26]
Occupied land assumed to be transformed land	-	-		[24]
Fuel burn efficiency	Constant			-
FT PtL-kerosene nomenclature	-	-		-
Environmental impacts of increasing the aromatic content of FT-PtL-kerosene	Ignored	-		[83,84]
Environmental impacts of transport: absolute values	Negligible	-		Postulated from [26]
Fuel combustion products constant until 2050	-	-		[29]
CO ₂ losses from CC plant outlet to final fuel	5%	[kg/kg]		Refer to literature in 2.2.
Feedstock CO ₂ to PtL-plant	0.07692	[kg/MJ]		-
Water recovery efficiency	90%	[kg/kg]		
Source of water, and location	Freshwater, Germany	-		[85]
Quality of freshwater	High	-		-
Freshwater abundance	Assumed	-		In line with [85]
Environmental impacts of water sourcing	Not included	-		-
SOEC	9.1	[kg/kg]		[44]
PEM	18.04	[kg/kg]		[44]
Deionizer (water conversion) efficiency	99%	[kg/kg]		[43]
Power converters and energy storage	Not included	-		-
Specific mass flows are identical in all PtL-plant layouts	-	-		Refer to 2.3. for details
Gas flare emissions	Negligible	-		[2]
Construction and EOL impacts of HTFT valid for LTFT plant as well	-	-		Refer to 2.3. for details
Operational life	20	[a]		[2]
Effect of excess heat recovery infrastructure on impacts	Negligible	-		-
Redirection of recycled hydrocarbons originally destined to burner to FT reactor	-	-		2.7.

Scalability of LCIA results of 300 MW CCGT plants to 50 MW Carbon Engineering CCGT plant	-	-	-
Land transformation from natural gas extraction, upstream	Considered	-	[86]
Water consumption	Negligible	-	[59]
Global Horizontal Irradiation	1,055	[kWh/(m ² a)]	[9]
Operational life	25	[a]	
Watt peak	200	[Wp]	
Module size	1.417	[m ²]	[13]
Conversion efficiency	16%	-	
Panel type	Poly-crystalline	-	[11]
	Flat plate array,		
Panel Tracking Type	without tracking.	-	[12]
Area requirement valid for all sizes	-	-	[65]
	Varies strongly across literature		
GWP-100 (per kWp)		-	[79]
Effects of transportation on environmental impacts	9%	on top of total	Refer to 2.11.1. for details
Capacity factor, Germany 2015	0.2063	-	Based on [87]
Operational life	20	[a]	
Turbine class	Onshore	-	
Nominal power	2	[MW]	
Plant size	50	[MW]	[7]
Generator type	Asynchronous	-	
Energy losses	Considered	-	
Technological readiness level (TRL)	≥ 5		[18]
Operational life	20	[a]	[54]
Climeworks plant: Impacts from infrastructure for additional heating	Negligible	-	By analogy with 2.3.
Water consumption, Carbon Engineering plant	4.7	[kg/kg]	[17]
Water consumption, Climeworks plant	Constant	-	[18]
Water consumption, Climeworks plant	Accounted as negative	-	-
Carbon Engineering plant: Impacts attributable to energy sources alone	Assumed	-	[17]

4. Break-even points of CO₂ eq. emissions of PtL-kerosene

Figure S12 shows the CO₂ eq. that the production electricity mix should have in order for the produced PtL-kerosene to have CO₂ eq. equal to Jet A-1 with (dark blue) and without considering non-CO₂ effects (light blue). Depending on the production pathway, the break-even point in which PtL-kerosene and Jet A-1 have the same CO₂ eq., ranges from 26.6 g CO₂ eq./MJ, electricity (layout producing the highest CO₂ eq.: LTFT combined with high-temperature DAC) to 61.8 g CO₂ eq./MJ, electricity (HTFT combined with low-temperature DAC). Furthermore, the differences between the break-even points for CO₂ eq. of PtL-kerosene measured in terms of GWP alone or GWP+RFI are low. Therefore, the GWP-100 of the electricity mix used in production has to be lower than 60.3 g CO₂ eq./kWh (not considering non-CO₂ effects) or 61.8 g CO₂ eq./kWh (considering non-CO₂ effects) for the layout HTFT and low-temperature DAC to deliver PtL-kerosene with lower CO₂ eq. than Jet A-1. For reference, the German grid mix in 2019 had a GWP-100 of 131.7 g CO₂ eq./MJ [88]. The break-even points for the layout producing the highest environmental impacts are (LTFT combined with high-temperature DAC) at a GWP-100 of the final electricity of 26.6 g CO₂ eq./MJ (not considering non-CO₂ effects), electricity and 27 g CO₂ eq./MJ, electricity (considering non-CO₂ effects).

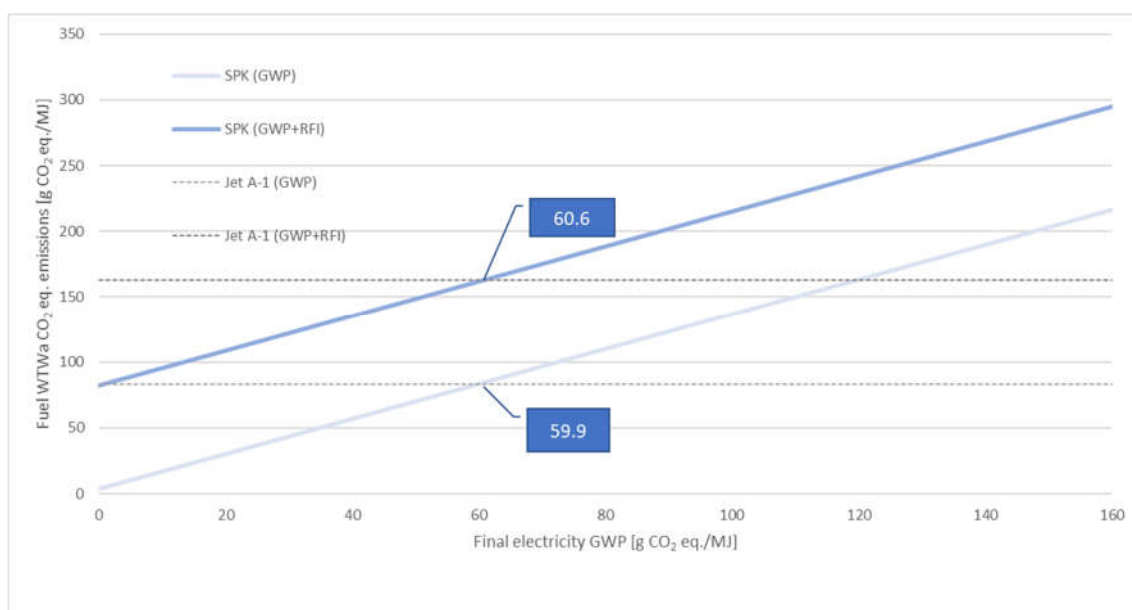


Figure S12. Break-even points of CO₂ eq. emissions of PtL-kerosene by GWP of final production electricity for the layout HTFT and low-temperature DAC (SPK = PtL-kerosene)

References

1. Simonen, K. *Life Cycle Assessment - Theory and Practice*; Hauschild, M.Z., Rosenbaum, R.K., Olsen, S.I., Eds.; Springer International Publishing: Cham, 2018; ISBN 978-3-319-56474-6.
2. Lozanovski, A.; Brandstetter, C.P. *Verbundprojekt Sunfire: Herstellung von Kraftstoffen Aus CO₂ Und H₂O Unter Nutzung Regenerativer Energie*; Stuttgart, Germany, 2015;
3. König, D.H.; Baucks, N.; Dietrich, R.U.; Wörner, A. Simulation and Evaluation of a Process Concept for the Generation of Synthetic Fuel from CO₂ and H₂. *Energy* **2015**, *91*, 833–841, doi:10.1016/j.energy.2015.08.099.
4. Cardarelli, F. *Materials Handbook - A Concise Desktop Reference*; Montreal, Canada, 2018; ISBN 9783319389233.
5. Sunfire GmbH Breakthrough for Power-to-X: Sunfire Puts First Co-Electrolysis into Operation and Starts Scaling Available online: <https://www.sunfire.de/en/company/news/detail/breakthrough-for-power-to-x-sunfire-puts-first-co-electrolysis-into-operation-and-starts-scaling> (accessed on 18 May 2020).
6. Plechinger, M. Vestas Challenging Germany's Market Leader Available online: <https://energywatch.eu/EnergyNews/Renewables/article11173088.ece> (accessed on 26 November 2019).
7. Razdan, P.; Garrett, P. *Life Cycle Assessment of Electricity Production from an Onshore V100-2 . 0 MW Wind Plant*; Aarhus, Denmark, 2015;
8. Wettengel, J. Last Major German Solar Cell Maker Surrenders to Chinese Competition Available online: <https://www.cleanenergywire.org/news/last-major-german-solar-cell-maker-surrenders-chinese-competition> (accessed on 4 December 2019).
9. Wirth, H. *Recent Facts about Photovoltaics in Germany*; Freiburg, Germany, 2017; Vol. 1;.
10. Hsu, E. China PV Powerhouses Profit Growth Hits All-Time High Available online: <https://www.energytrend.com/news/20191015-15437.html> (accessed on 4 December 2019).
11. Fraunhofer Institute for Solar Energy Systems *Photovoltaics Report 2019*; Freiburg, Germany, 2019;
12. US department of energy *Developing Clean Energy Projects on Tribal Lands - Data and Resources for Tribes*; Washington, DC, USA, 2012;
13. Fu, Y.; Liu, X.; Yuan, Z. Life-Cycle Assessment of Multi-Crystalline Photovoltaic Systems in China. *J. Clean. Prod.* **2014**, *86*, 180–190, doi:10.1016/j.jclepro.2014.07.057.
14. Sphera Life Cycle Assessment Software (GaBi Ts) Available online: <https://sphera.com/life-cycle-assessment-software-download/> (accessed on 19 April 2022).
15. Schüwer, D.; Hanke, T.; Luhmann, H.-J. *Konsistenz Und Aussagefähigkeit Der Primärenergie-Faktoren Für Endenergieträger Im Rahmen Der EnEV*; Wuppertal, Germany, 2015;
16. Bauknecht, D.; Preuschoff, S. *Ökobilanzen Für Den Sektor Strom Und Gas*; Jülich, Germany, 2006;
17. Keith, D.W.; Holmes, G.; St. Angelo, D.; Heidel, K. A Process for Capturing CO₂ from the Atmosphere. *Joule* **2018**, 1573–1594, doi:10.1016/j.joule.2018.05.006.
18. Viebahn, P.; Scholz, A.; Zelt, O. The Potential Role of Direct Air Capture in the German Energy Research Program—Results of a Multi-Dimensional Analysis. *Energies* **2019**, *12*, 3443, doi:10.3390/en12183443.
19. Bester, N.; Yates, A. Assessment of the Operational Performance of Fischer-Tropsch Synthetic-Paraffinic Kerosene in a T63 Gas Turbine Compared to Conventional Jet A-1 Fuel. In Proceedings of the ASME Turbo

Expo; Orlando, FL, USA, 2009; Vol. 2, pp. 1063–1077.

20. Lee, D.S.; Pitari, G.; Grewe, V.; Gierens, K.; Penner, J.E.; Petzold, A.; Prather, M.J.; Schumann, U.; Bais, A.; Bernsten, T.; et al. Transport Impacts on Atmosphere and Climate: Aviation. *Atmos. Environ.* **2010**, *44*, 4678–4734, doi:10.1016/j.atmosenv.2009.06.005.
21. Masiol, M.; Harrison, R.M. Aircraft Engine Exhaust Emissions and Other Airport-Related Contributions to Ambient Air Pollution: A Review. *Atmos. Environ.* **2014**, *95*, 409–455, doi:10.1016/j.atmosenv.2014.05.070.
22. Stratton, R.W.; Wolfe, P.J.; Hileman, J.I. Impact of Aviation Non-CO₂ Combustion Effects on the Environmental Feasibility of Alternative Jet Fuels. *Environ. Sci. Technol.* **2011**, *45*, 10736–10743, doi:10.1021/es2017522.
23. Jungbluth, N.; Meili, C. Recommendations for Calculation of the Global Warming Potential of Aviation Including the Radiative Forcing Index. *Int. J. Life Cycle Assess.* **2019**, *24*, 404–411, doi:10.1007/s11367-018-1556-3.
24. Bos, U. *Documentation of Land Use Inventory in GaBi*; Leinfelden-Echterdingen, Germany, 2018;
25. Federal Ministry of Food and Agriculture *Bioenergy in Germany : Facts and Figures - Solid Fuels, Biofuels & Biogas*; Berlin, Germany, 2019;
26. Elgowainy, A.; Han, J.; Wang, M.; Carter, N.; Stratton, R.; Hileman, J.; Malwitz, A.; Balasubramanian, S. *Life-Cycle Analysis of Alternative Aviation Fuels in GREET*; Oak Ridge, TN, USA, 2012;
27. Schuller, O. *The GaBi Refinery Model*; Leinfelden-Echterdingen, Germany, 2019;
28. FAO AQUASTAT Main Database Available online: <http://www.fao.org/nr/water/aquastat/data/query/index.html?lang=en> (accessed on 3 December 2019).
29. Jiang, H. *Key Findings on Airplane Economic Life - Boeing Commercial Airplanes*; Seattle, WA, USA, 2013;
30. Sphera Process Data Set: Kerosene / Jet A1 at Refinery; from Crude Oil; Production Mix, at Refinery; 400 Ppm Sulphur (En) Available online: <http://gabi-documentation-2019.gabi-software.com/xml-data/processes/6c664f4e-833b-4468-acc5-2ba81a1c6c4a.xml> (accessed on 7 February 2020).
31. Searle, S.; Christensen, A. *Decarbonization Potential of Electrofuels in the European Union, an ICCT White Paper*; Washington, DC, USA, 2018;
32. Deutsche Energie-Agentur GmbH (dena) *Powerfuels : Missing Link to a Successful Global Energy Transition Current State of Technologies , Markets , and Politics – and Start of a Global Dialogue*; 2019;
33. Future market insights Hydrogen Electrolyzer Market - Global Industry Analysis, Size and Forecast, 2018 to 2028 Available online: <https://www.persistencemarketresearch.com/market-research/hydrogen-electrolyzer-market.asp> (accessed on 7 February 2020).
34. Navigant *Electrolyzers - Water Electrolysis Units for Industry, Transportation, and Energy Storage*; 2019;
35. Alfa Laval *Environmental Product Declaration: Plate Heat Exchanger*; 2017;
36. Fasihi, M.; Bogdanov, D.; Breyer, C. Techno-Economic Assessment of Power-to-Liquids (PtL) Fuels Production and Global Trading Based on Hybrid PV-Wind Power Plants. *Energy Procedia* **2016**, *99*, 243–268, doi:10.1016/j.egypro.2016.10.115.
37. Posdziech, O.; Stäber, R.; von Olshausen, C. *Synfuels from Electrolysis/Sunfire*; Dresden, Germany, 2017;
38. Lupi, S. *Fundamentals of Electroheat*; Springer International Publishing: Cham, Switzerland, 2017; ISBN 978-3-319-46014-7.
39. Wattco Technical Specifications of Wattco Flange Heaters 2020.

40. Bustamante, F.; Enick, R.M.; Cugini, A. V.; Killmeyer, R.P.; Howard, B.H.; Rothenberger, K.S.; Ciocco, M. V.; Morreale, B.D.; Chattopadhyay, S.; Shi, S. High-Temperature Kinetics of the Homogeneous Reverse Water-Gas Shift Reaction. *AIChE J.* **2004**, *50*, 1028–1041, doi:10.1002/aic.10099.
41. Fakheri, A. Heat Exchanger Efficiency. *J. Heat Transfer* **2007**, *129*, 1268–1276, doi:10.1115/1.2739620.
42. Koj, J.C.; Wulf, C.; Schreiber, A.; Zapp, P. Site-Dependent Environmental Impacts of Industrial Hydrogen Production by Alkaline Water Electrolysis. *Energies* **2017**, *10*, doi:10.3390/en10070860.
43. Anderson, M.A.; Cudero, A.L.; Palma, J. Capacitive Deionization as an Electrochemical Means of Saving Energy and Delivering Clean Water. Comparison to Present Desalination Practices: Will It Compete? *Electrochim. Acta* 2010.
44. Mehmeti, A.; Angelis-Dimakis, A.; Arampatzis, G.; McPhail, S.; Ulgiati, S. Life Cycle Assessment and Water Footprint of Hydrogen Production Methods: From Conventional to Emerging Technologies. *Environments* **2018**, *5*, 24, doi:10.3390/environments5020024.
45. Hasanbeigi, A.; Arens, M.; Cardenas, J.C.R.; Price, L.; Triolo, R. Comparison of Carbon Dioxide Emissions Intensity of Steel Production in China, Germany, Mexico, and the United States. *Resour. Conserv. Recycl.* **2016**, *113*, 127–139, doi:10.1016/j.resconrec.2016.06.008.
46. Verein Deutscher Zementwerke *Monitoring Bericht: Verminderung Der CO2 Emissionen*; Düsseldorf, Germany, 1998;
47. Andrew, R.M. Global CO2 Emissions from Cement Production, 1928-2018. *Earth Syst. Sci. Data* 2019, *11*, 1675–1710.
48. European Aluminum Association *Aluminium Recycling in LCA*; Brussels, Belgium, 2013;
49. World Steel Association Steel Confirmed as Most Recycled Packaging Material in Two Regions of the World Available online: <https://web.archive.org/web/20160412121055/https://www.worldsteel.org/media-centre/Steel-news/Steel-confirmed-as-most-recycled-packaging-material-in-two-regions-of-the-world.html> (accessed on 5 January 2020).
50. Lundberg, S. Comparative LCA of Electrolyzers for Hydrogen Gas Production, Master Thesis, KTH Royal Institute of Technology, Stockholm, Sweden, 2019.
51. Keith, D.W.; Holmes, G.; St. Angelo, D.; Heidel, K. A Process for Capturing CO2 from the Atmosphere. *Joule* **2018**, *2*, 1573–1594, doi:10.1016/j.joule.2018.05.006.
52. Holmes, G.; Keith, D.W. An Air-Liquid Contactor for Large-Scale Capture of CO2 from Air. *Philos. Trans. R. Soc. A Math. Phys. Eng. Sci.* **2012**, doi:10.1098/rsta.2012.0137.
53. Smith, P.; Davis, S.J.; Creutzig, F.; Fuss, S.; Minx, J.; Gabrielle, B.; Kato, E.; Jackson, R.B.; Cowie, A.; Kriegler, E.; et al. Biophysical and Economic Limits to Negative CO2 Emissions. *Nat. Clim. Chang.* **2016**, *6*, 42–50, doi:10.1038/nclimate2870.
54. Fasihi, M.; Efimova, O.; Breyer, C. Techno-Economic Assessment of CO2 Direct Air Capture Plants. *J. Clean. Prod.* **2019**, *224*, 957–980, doi:10.1016/j.jclepro.2019.03.086.
55. Sphera Solutions GmbH Sphera GaBi Product Sustainability Software 2021.
56. König, D.H. Techno - Ökonomische Prozessbewertung Der Herstellung Synthetischen Flugturbinentreibstoffes Aus CO2 Und H2, Dissertation, University of Stuttgart, Stuttgart, Germany, 2016.
57. Şencan Şahin, A.; Kiliç, B.; Kiliç, U. Design and Economic Optimization of Shell and Tube Heat Exchangers Using Artificial Bee Colony (ABC) Algorithm. *Energy Convers. Manag.* **2011**, *52*, 3356–3362, doi:10.1016/j.enconman.2011.07.003.

58. Climeworks Our Products | Climeworks – Capturing CO₂ from Air Available online: <https://www.climeworks.com/our-products/> (accessed on 12 March 2020).
59. Mielke, E.; Diaz Anadon, L.; Narayanamurti, V. Water Consumption of Energy Resource Extraction, Processing, and Conversion. *Harvard Kennedy Sch. Energy Technol. Innov. Policy Discuss. Pap. Ser.* **2010**, 52, doi:Discussion Paper No. 2010-15.
60. Bradsher, K. Hauling New Treasure Along the Silk Road Available online: <https://www.nytimes.com/2013/07/21/business/global/hauling-new-treasure-along-the-silk-road.html> (accessed on 3 December 2019).
61. Oltermann, P. Germany's "China City": How Duisburg Became Xi Jinping's Gateway to Europe Available online: <https://www.theguardian.com/cities/2018/aug/01/germanys-china-city-duisburg-became-xi-jinping-gateway-europe> (accessed on 3 December 2019).
62. European Environment Agency Specific CO₂ Emissions per Tonne-Km and per Mode of Transport in Europe, 1995-2011 Available online: <https://www.eea.europa.eu/data-and-maps/figures/specific-co2-emissions-per-tonne-2> (accessed on 5 February 2020).
63. International Energy Agency China -Electricity Generation by Source, 1990-2017 Available online: <https://www.iea.org/countries/china> (accessed on 3 December 2019).
64. International Energy Agency Europe – Electricity Generation by Source, 1990-2017 Available online: <https://www.iea.org/regions/europe> (accessed on 3 December 2019).
65. Ong, S.; Campbell, C.; Denholm, P.; Margolis, R.; Heath, G.; Ong, S.; Campbell, C.; Denholm, P.; Margolis, R.; Heath, G. *Land-Use Requirements for Solar Power Plants in the United States Land-Use Requirements for Solar Power Plants in the United States*; Golden, Colorado, 2013;
66. Hau, E. *Wind Turbines - Fundamentals, Technologies, Application, Economics; 2nd Edition*; Springer: Heidelberg, Germany, 2006;
67. Denholm, P.; Jackson, M.; Ong, S.; Hand, M. *Land-Use Requirements of Modern Wind Power Plants in the United States/NREL*; Golden, Colorado, 2009;
68. Eymann, L.; Stucki, M.; Fürholz, A.; König, A. *Ökobilanzierung von Schweizer Windenergie*; Wädenswil, Switzerland, 2015;
69. Rohrig, K. *Windenergie Report Deutschland 2017*; Stuttgart, Germany, 2018;
70. German Wind Energy Association *BWE Industry Report: Wind Industry in Germany 2015*; Berlin, Germany, 2018;
71. Wehrmann, B. Design of Germany's Wind Power Distance Rules Undecided as Opposition to Policy Grows Available online: <https://www.cleanenergywire.org/news/design-germanys-wind-power-distance-rules-undecided-vexation-over-policy-grows> (accessed on 15 March 2020).
72. Kinder, J.D.; Rahmes, T. *Evaluation of Bio-Derived Synthetic Paraffinic Kerosene - The Boeing Company*; Seattle, WA, USA, 2009;
73. CML-Department of Industrial Ecology CML-IA Characterisation Factors Available online: <https://www.universiteitleiden.nl/en/research/research-output/science/cml-ia-characterisation-factors#downloads> (accessed on 16 December 2019).
74. CML - Department of Industrial Ecology *CML-IA Characterisation Factors*; Institute of the Faculty of Science of Leiden University: Leiden, The Netherlands, 2021;
75. European Commission *Best Available Techniques (BAT) Reference Document for the Refining of Mineral Oil and Gas*; Brussels, Belgium, 2015;

76. Defilippi, E. The Environmental Cost of Peru's Domestic Air Transport: An Appraisal. *J. Air Transp. Manag.* **2019**, *78*, 144–151, doi:10.1016/j.jairtraman.2019.01.008.
77. Mazareanu, E. Commercial Airlines: Worldwide Fuel Consumption 2019 Available online: <https://www.statista.com/statistics/655057/fuel-consumption-of-airlines-worldwide/> (accessed on 20 March 2020).
78. Jensen, J.O.; Jensen, S.H.; Tophøj, N. *Pre-Investigation of Water Electrolysis*; Lyngby, Denmark, 2008;
79. Gerbinet, S.; Belboom, S.; Léonard, A. Life Cycle Analysis (LCA) of Photovoltaic Panels : A Review. *Renew. Sustain. Energy Rev.* **2014**, *38*, 747–753, doi:10.1016/j.rser.2014.07.043.
80. International Energy Agency Oil Final Consumption by Product - Retired Database Available online: <https://www.iea.org/classicstats/statisticssearch/report/?country=WORLD&product=oil&year=2015> (accessed on 12 September 2019).
81. Royal Dutch Shell *Jet A-1 Safety Data Sheet - Regulation 1907/2006/EC*; Hamburg, Germany, 2018;
82. Linde Gas GmbH *Rechnen Sie Mit Wasserstoff. Die Datentabelle.*; Stadl-Paura, Austria, 2013;
83. Liu, G.; Yan, B.; Chen, G. Technical Review on Jet Fuel Production. *Renew. Sustain. Energy Rev.* **2013**, *25*, 59–70, doi:10.1016/j.rser.2013.03.025.
84. Klerk, A. De Fischer-Tropsch Fuels Refinery Design. *Energy Environ. Sci.* **2011**, *4*, 1177–1205, doi:10.1039/c0ee00692k.
85. German Association of Energy and Water Industries *Profile of the German Water Industry*; Bonn, Germany, 2008;
86. Thinkstep GaBi Ts (Demo Database) 2019.
87. Fraunhofer Institute Fraunhofer Energy Charts Available online: <https://www.energy-charts.de/> (accessed on 9 February 2019).
88. Icha, P.; Kugs, G. *Entwicklung Der Spezifischen Kohlendioxid-Emissionen Des Deutschen Strommix in Den Jahren 1990-2018*; Berlin, Germany, 2019;
89. Schmidt, P.; Weindorf, W.; Raksha, T.; Wurster, R.; Bittel, H.; Lanoix, J.-C. *Future Fuel for Road Freight – Techno-Economic & Environmental Performance Comparison of GHG-Neutral Fuels & Drivetrains for Heavy-Duty Trucks*; Munich, DE/Brussels, BE/Paris, FR, 2019;
90. Gopal, E.S.R. Specific Heats of Gases. In *Specific Heats at Low Temperatures*; Springer US: Boston, MA, 1966; pp. 135–157.
91. Wang, T. Global Offshore Wind Power Market Available online: <https://www.statista.com/topics/2764/offshore-wind-energy/> (accessed on 10 December 2019).
92. Wang, T. Global Wind Power Market Available online: <https://www.statista.com/topics/4564/global-wind-energy/> (accessed on 10 December 2019).
93. International Energy Agency Offshore Wind Outlook 2019 Available online: <https://www.iea.org/reports/offshore-wind-outlook-2019> (accessed on 10 December 2019).